

Article

The Earliest Clastic Sediments of the Xiong'er Group: Implications for the Early Mesoproterozoic Sediment Source System of the Southern North China Craton

Yuan Zhang ^{*}, Guocheng Zhang and Fengyu Sun 

School of Resources and Environment, Henan Polytechnic University, Jiaozuo 454003, China

^{*} Correspondence: zy3519718@163.com

Abstract: The volcanic activity of the Xiong'er Group and its concomitant sedimentation are related to the stretching–breakup of the Columbia supercontinent. The Dagushi Formation overlies the Paleoproterozoic Shuangfang Formation with an angular unconformity. The Dagushi Formation, as the earliest clastic strata of the Xiong'er Group and the first stable sedimentary cover overlying the Archean crystalline basement in the southern margin of the North China Craton, provides tectonic evolution information that predates Xiong'er volcanic activity. By distinguishing lithologic characteristics and sedimentary structures, we identified that the sedimentary facies of the Dagushi Formation were braided river delta lake facies from bottom to top. The U–Pb ages of the detrital zircons of the Dagushi Formation can be divided into four groups: ~1905–1925, ~2154–2295, ~2529–2536, and ~2713–2720 Ma, indicating the provenance from the North China Craton basement. Based on the geochemical characteristics of the Dagushi Formation, we suggest that the sediments accumulated rapidly near the source, which were principally felsic in nature, and were supplemented by recycled materials. The provenance area pointed to the underlying metamorphic crystalline basement of the North China Craton as the main source area with an active tectonic background. The Chemical Index of Alteration (CIA) values of the Dagushi Formation sandstone samples ranged from 60.8 to 76.7, indicating that the source rocks suffered from slight to moderate chemical weathering. The Index of Composition Variability (ICV) values ranged from 0.8 to 1.3, which indicates the first cyclic sediments. The vertical facies and provenance changes of the Dagushi Formation reflect a continuous crust fracturing process that occurred in the North China Craton.

Keywords: North China Craton; Dagushi Formation; sedimentary facies; detrital zircon; geochemistry



Citation: Zhang, Y.; Zhang, G.; Sun, F. The Earliest Clastic Sediments of the Xiong'er Group: Implications for the Early Mesoproterozoic Sediment Source System of the Southern North China Craton. *Minerals* **2023**, *13*, 971. <https://doi.org/10.3390/min13070971>

Academic Editors: Georgia Pe-Piper, Jin Liu, Jiahui Qian and Xiaoguang Liu

Received: 8 June 2023

Revised: 15 July 2023

Accepted: 17 July 2023

Published: 22 July 2023



Copyright: © 2023 by the authors. Licensee MDPI, Basel, Switzerland. This article is an open access article distributed under the terms and conditions of the Creative Commons Attribution (CC BY) license (<https://creativecommons.org/licenses/by/4.0/>).

1. Introduction

The North China Craton (NCC) is an ancient landmass with a long history covering 3.8 billion years, with evidence concerning many supercontinent events in geological history [1–6], including assembly and breakup records of the supercontinent Columbia [7–10]. Scholars think that the subduction between the eastern and western blocks occurred at ca. 1850 Ma, thus forming a unified NCC [11–14]. After that, a volcanic sedimentary succession, which is called the Xiong'er Group, was widely developed in the southern margin of the NCC. The Xiong'er Group can be divided from bottom to top into the Dagushi Formation, Xushan Formation, Jidanping Formation, and Majiahe Formation, which are a set of clastic rock and volcanic strata with low deformation and metamorphism. In recent years, scholars have conducted extensive research on the Xiong'er Group in the southern margin of the NCC using petrology, geochemistry, and chronology [6,9,12,15–35] (Figure 1a). The chronological data of zircon uranium-lead (U–Pb) isotopes show that most of the volcanic rocks of the Xiong'er Group were formed between 1800 and 1750 Ma [24,30]. However, the formation mechanism remains controversial [9,15–20]. To date, the main viewpoints include an Andean-type continental margin [9,22], a passive continental margin and rift [26–28,36,37], and an active continental margin and rift [22].

However, research on the Xiong'er Group has focused on its volcanic lavas, while the sedimentary rocks have not been a major subject of systematic research. Only a few scholars have investigated the geochemical characteristics of the clastic rocks from the Dagushi Formation [38]. Ref. [39] posited that the existence of primary glauconite in the sandstone of the Majiahe Formation proved that the Xiong'er Group was in a marine environment during its later stage. There is also controversy concerning the sedimentary source, which limits the correlation between the Mesoproterozoic strata in the southern margin of the NCC and other regions. Therefore, studies on the sedimentary environment, provenance characteristics, and tectonic setting of early Mesoproterozoic strata in the southern margin of the NCC are critical to reveal the evolution of paleogeography during the Proterozoic eon (Figure 1b,c). schematic diagram of the geographical location of the Dagushi Formation in the study area (modified from [40,41]).

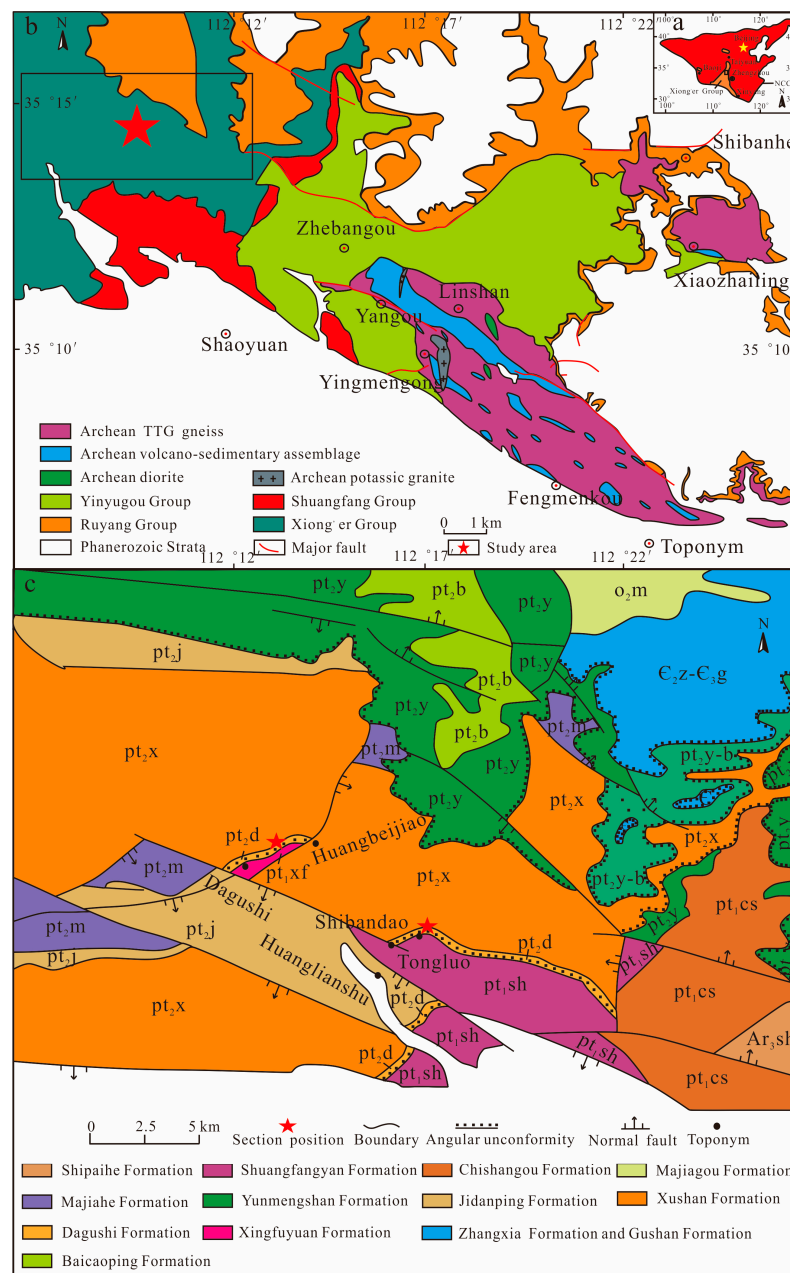


Figure 1. (a) Geological distribution of the Xiong'er Group in the NCC during the Precambrian era (modified from [19]); (b) simplified geological map of the study area (modified from [40]); (c).

2. Geological Background

The total area of the NCC is approximately 1.6 million km². Important components include northern China, Bohai Bay, and Inner Mongolia [42,43]. The NCC has a long history of geological evolution and has experienced several multi-stage tectonic evolution events [5,26,44–49]. Furthermore, the formation of the NCC has experienced three important geological events: the main continental crust growth at ~2.7 Ga, the cratonization event at ~2.5 Ga, and the final formation of the NCC at ~2.0–1.8 Ga [42,50,51].

The Xiong'er Group is primarily exposed in the Zhongtiao, Xiao, Xiong'er, and Waifang mountains [25,52]. The Xiong'er Group, as the cover of an ancient continental crust basement, overlies the Archean crystalline basement or early Proterozoic strata with an unconformity [53]. They represent the most extensive magmatic activity that occurred after the formation of the crystalline basement in the NCC [38,52]. The volcanic rocks are primarily andesite and basaltic andesite, with a small amount of dacite, rhyolite, and minor interlayered sedimentary rocks. Sedimentary rocks, sedimentary interbeds, and pyroclastic rocks are limited, covering only 4.3% of the total thickness of the layer, and mainly distributed in the Dagushi Formation at the bottom and the Majiahe Formation at the top, while only a small number of local intervals are exposed in the Xushan and Jidanping Formations [24,38,54].

The outcrop range of sedimentary rocks in the Dagushi Formation is small, and the thickness varies greatly. The representative section is located in Huangbeijiao and Xiaogoubei in Shaoyuan Town, Jiyuan City, Henan Province. The Dagushi Formation in this area overlays the biotite quartz schist of the late Neoproterozoic Shuangfang Formation with an angular unconformity, and its distribution is continuous, and its largest thickness is 189.5 m. The Dagushi Formation is also distributed in Moshigou, northern Luanchuan County, with a maximum thickness of 92 m. The main lithology is as follows: conglomerate, arkose sandstone, feldspathic quartz sandstone, and purple mudstone. Cross-bedding is developed in sandstone strata. In addition, the Dagushi Formation in eastern Yuanqu County of Shanxi Province and Luoning County of Henan Province outcrops sporadically. In this study, the Dagushi Formation, which is completely exposed in Huangbeijiao and Xiaogoubei north of Shaoyuan Town, Jiyuan City, was selected as the research object (Figure 1c).

3. Analytical Methods

Two coarse- to medium-grained sandstone samples (approximately 4 kg) were collected from the lowest and uppermost parts of the Dagushi Formation within the Huangbeijiao section in Jiyuan City, southern North China, for zircon separation (Figures 1 and 2). Zircon was separated using a heavy fluid and magnetic separator at the Hebei Institute of Regional Geology and Mineral Resources, Langfang, China. Approximately 400 zircons were hand-selected from each sample using a binocular microscope, and 177 zircons were selected to analyze. Zircon particles were attached to adhesive tape with M257 standard [55], sealed with epoxy resin, and polished to half of their thickness. The images of these zircons were taken using an optical microscope with transmitted and reflected light. High-resolution cathodoluminescence imaging was performed by a scanning electron microscope using the Gatan monoCL 3 + cathodoluminescence system from Wuhan SampleSolution Analytical Technology Co., Ltd. (Wuhan, China). Both imaging methods were used to identify internal structures and select targets for further U–Pb analysis.

U–Pb dating and zircon trace element analysis were conducted simultaneously by laser ablation inductively coupled plasma mass spectrometry (ICP-MS). Detailed operating parameters and procedures for laser ablation systems, ICP-MS instruments (Wuhan SampleSolution Analytical Technology Co., Ltd.), and data simplification can be found in [56–58]. Laser sampling was performed using a GeoLas 2005 instrument, and an Agilent 7900 ICP-MS system (Agilent Technologies, Palo Alto, CA, USA) was used to obtain the ion signal strength. A laser beam repetition rate of 5 Hz and an analysis point size of 24 µm diameter were used for each analysis. Helium was used as a carrier gas, and argon was used

as a supplementary gas. Before entering the ICP, the sample was mixed with the carrier gas through a T-joint. The laser is equipped with an ablation system to smooth the signal, which can produce a smooth signal even at very low temperatures and frequencies [59] (i.e., down to 1 Hz). Each analysis consisted of approximately 20 s of background acquisition and 30 s of gas blank, followed by 50 s of sample data acquisition. The Excel-based software, ICPMSDataCal (Ver. 10.0), performed the offline selection, unified background and signal analysis, time trend correction of the records, quantitative element correction analysis, and U–Pb dating [56,57,60].

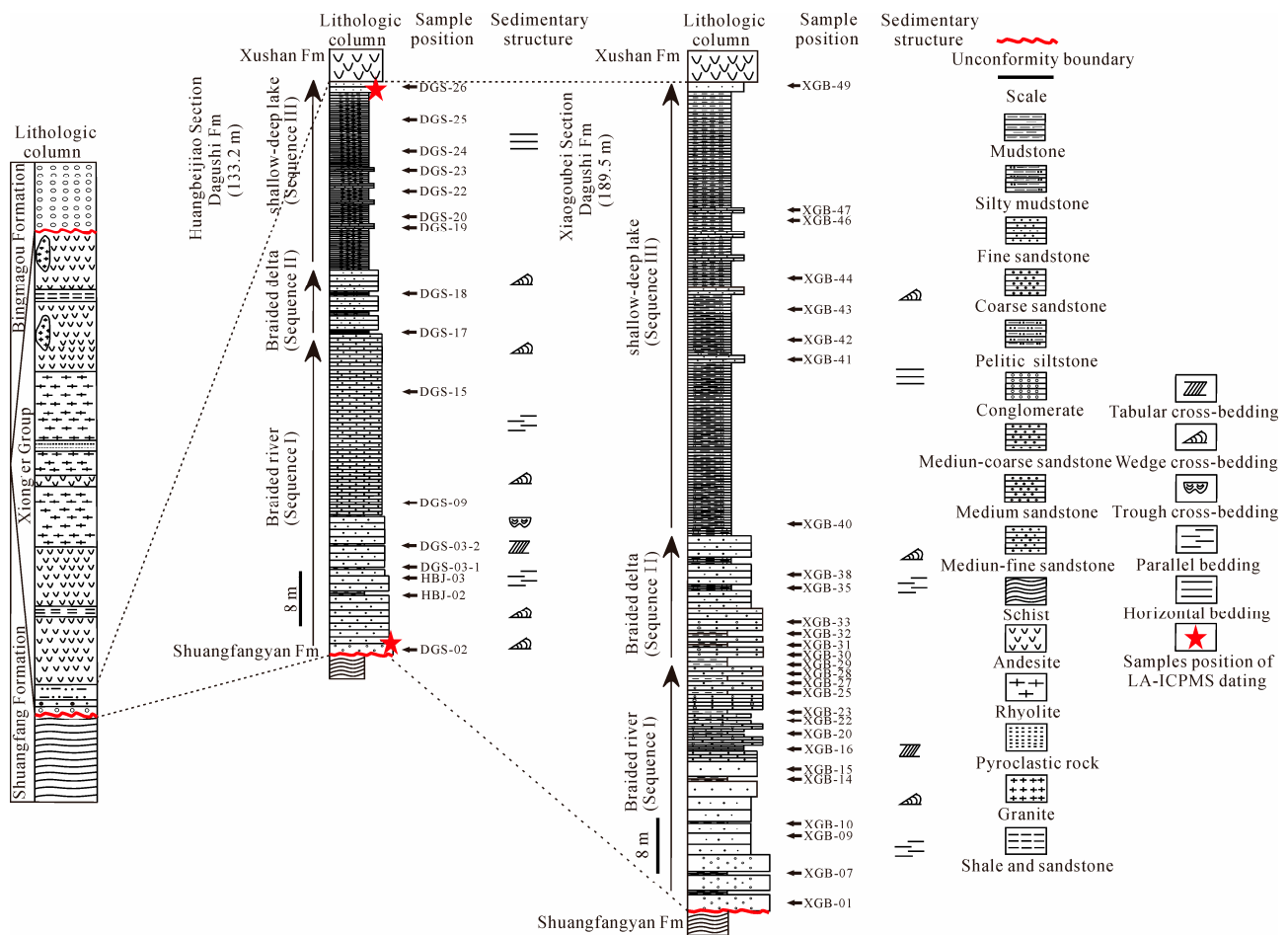


Figure 2. Generalized column of the Mesoproterozoic Dagushi Formation in Jiyuan (this study).

The standard zircon 91,500 was used for U–Pb dating, and two determinations were analyzed for every five measurements. The variation of the U–Th–Pb isotope ratio with time was corrected for every five analyses by linear interpolation [57,58]. The standard preferred U–Th–Pb isotope ratio for 91,500 was taken from [61]. The $^{207}\text{Pb}/^{206}\text{Pb}$ age was used for zircons greater than 1000 Ma [62]. For zircons less than 1000 Ma, the discordance was defined as $100\% \times \text{abs} [1 - (^{206}\text{Pb}/^{238}\text{U}) / (^{207}\text{Pb}/^{235}\text{U})]$, and for zircons greater than 1000 Ma, the discordance was defined as $100\% \times \text{abs} [1 - (^{206}\text{Pb}/^{238}\text{Pb}) / (^{207}\text{Pb}/^{206}\text{Pb})]$. Harmonic graphs were then generated, and the weighted average was determined using Isoplot/Ex_ver3 software [63].

Samples were collected from sandstone and argillaceous rocks from the Dagushi Formation in the Jiyuan area for geochemical analysis, and major elements in the sandstone and trace elements in the argillaceous rocks were determined. After the sample was naturally dried, it was crushed into a 200-mesh powder using a mortar. An Axios^{max} X-ray fluorescence (XRF) spectrometer (PANalytical BV, Almelo, the Netherlands) was used in a laboratory at ALS Minerals-ALS Chemex (Guangzhou, China) Co., Ltd. in Guangdong

Province. The whole rock major element described the detailed analysis procedure with errors between $\pm 1\%$ and $\pm 2\%$ [64].

Trace elements, including rare earth elements (REE), were detected by an Agilent 7900 ICP-MS Inductively Coupled Plasma Mass Spectrometer in ALS Minerals-ALS Chemex (Guangzhou, China) Co., Ltd. The analytical accuracy of trace elements exceeded 95%, and the detection range was less than or equal to 2 ppm in most cases. The detection range of Ba, Cr, Rb, Sr, and V was 5 ppm.

4. Results

4.1. Sedimentary Facies

We researched two sections of strata from the Mesoproterozoic Dagushi Formation in the Jiyuan area, divided their sedimentary facies, and further analyzed their sedimentary environment. Our measurements showed that the thickness of the Huangbeijiao Section from the Dagushi Formation in the Jiyuan area was approximately 133.2 m, while the thickness of the Xiaogoubei Section was 189.5 m (Figure 2). Our field observations showed that the Dagushi Formation rested upon the Paleoproterozoic crystalline basement unconformably and was the only sedimentary rock stratum in the Xiong'er Group. The color, composition, and structural characteristics of sediments in this stratum had distinct variations. In general, this stratum was a retrograding sequence which consisted of three different sedimentary sequences from bottom to top (Figure 2). Each sequence is summarized and described below.

Huangbeijiao Section (133.2 m).

Sequence I (71.4 m): the lithology of Sequence I in the Huangbeijiao Section was gray and purple pebbly sandstone and medium- to coarse-grained sandstone. From bottom to top, the grain size of sediments changed from coarse to fine with a positive rhythm, and the roundness changed from subangular to subrounded. Sequence I had parallel bedding formed by water ripple and large cross-bedding (Figure 3a–d) which occurred repeatedly from bottom to top. Sandstone layers with different grain sizes constituted multiple sedimentary cycles, and lenticular sand bodies were observed (Figure 3e). Based on the lithologic characteristics and recognizable sedimentary structures, Sequence I exhibited characteristics of a braided river deposit.

Sequence II (17.5 m): the lithology of Sequence II in the Huangbeijiao Section was primarily interbedding formed by purple medium- to fine-grained sandstone, siltstone, and mudstone (Figure 3f). The grain size was significantly smaller than that of Sequence I, and the main bedding was small wedge-shaped cross-bedding (Figure 3g). Irregular horizontal bedding was occasionally seen in the mudstone layers, and mud cracks were developed in the bedding of the local mudstone layers (Figure 3h). Mud cracks were most common in dry areas, and they were formed after silty or argillaceous sediments exposed their water surface, lost water, became dry, and shrank, which indicated exposure to a dry environment. Sequence II was thought to be a braided delta deposit.

Sequence III (44.3 m): the lithology of Sequence III in the Huangbeijiao Section was purple argillaceous siltstone and mudstone, which were typical products of overbank deposition. A significant amount of the rocks was severely weathered (Figure 3i), and there was no sedimentary structure of fluvial origin. The lithology in this sequence began to significantly change, and a great number of argillaceous sediments occurred. Compared to Sequence II, the grain size continued to decrease. The roundness of the sediment grains was mainly subrounded and occasionally subangular. Sequence III was thought to be a shore shallow lake deposit with weak hydrokinetics and without stagnancy.

Xiaogoubei Section (189.5 m).

Sequence I (71.6 m): the lithology of Sequence I in the Xiaogoubei Section was an interbedding of light purple medium- to thick-bedded, medium- to fine-grained sandstone and brown thin-bedded argillaceous rock. The basal sandstone included gravel with a diameter range from millimeters to centimeters which reflected a process in which sediments accumulated rapidly after short-distance transportation. From bottom to top,

this sequence demonstrated multiple normal cycle rhythmites that were thick at the bottom and thin at the top. At the bottom of each cycle, there were pronounced scouring surfaces and coarse-grained imbricated pebbly sandstone layers (Figure 4a). The sandstone layer in the lower part of the cycle was characterized by large wedge- and trough-shaped cross-bedding, graded bedding, and parallel bedding, and lenticular sand bodies were commonly seen, which were flat at the top and convex at the bottom (Figure 4b–d). The siltstone or argillaceous siltstone in the upper part of the cycle was primarily small cross-bedding and wavy bedding, suggesting that it belonged to a braided river deposit with a strong hydrodynamic force that was controlled by directional flow in shallow water.

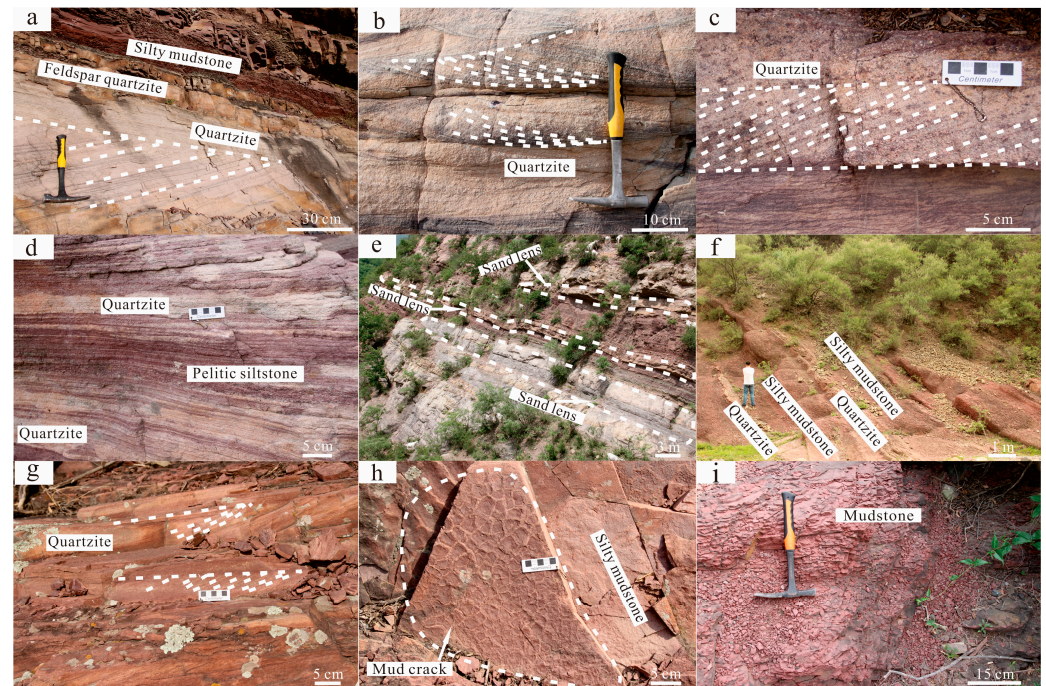


Figure 3. Lithologic characteristics and sedimentary structure of the Dagushi Formation in the Huang-beijiao section of Jiyuan. (a) Wedge-shaped cross-bedding; (b) trough cross-bedding; (c) tabular cross-bedding; (d) parallel bedding; (e) sand lens; (f) lithology characteristics of section II; (g) small wedge cross-bedding; (h) mud crack structure; (i) lithology characteristics of section III.

Sequence II (22 m): the lithology of Sequence II in the Xiaogoubei Section was a shallow conglomerate with medium thickness and pebbly coarse sandstone at the bottom, an interbedding of purple medium-grained sandstone and purple sandy mudstone in the middle, and purple and gray–green silty mudstone at the top. The basal scouring surface had a gentle slope, and the conglomerate, pebbled coarse sandstone, and sandstone all exhibited low compositional and textural maturity with mixed sizing (Figure 4e). The grain size of the sediments was significantly attenuated from bottom to top. Medium and small cross-bedding, parallel bedding, and lateral accretion cross-bedding were developed (Figure 4f,g). The sizes of various beds were smaller than those of Sequence I, suggesting that the hydrodynamics shifted from strong to weak and the water turbulence increased. Sequence II was determined to be a braided delta deposit.

Sequence III (95.9 m): the lithology included amaranth medium- to thick-bedded argillaceous siltstone at the bottom, the interbedding of thick-bedded purple argillaceous siltstone and mudstone in the middle, and gray–green coarse sandstone at the top. The compositional maturity, sizing, and roundness of the clastic material were better than those of Sequence II, and there was no sedimentary structure of fluvial origin; however, there was irregular horizontal bedding in local areas (Figure 4h), which indicated weak hydrodynamics. In addition to outcropped coarse sandstone at the top, the sediments of

Sequence III were mostly fine-grained silty and argillaceous sediments, indicating that the water gradually deepened. Thus, Sequence III was thought to be a shore shallow lake deposit.

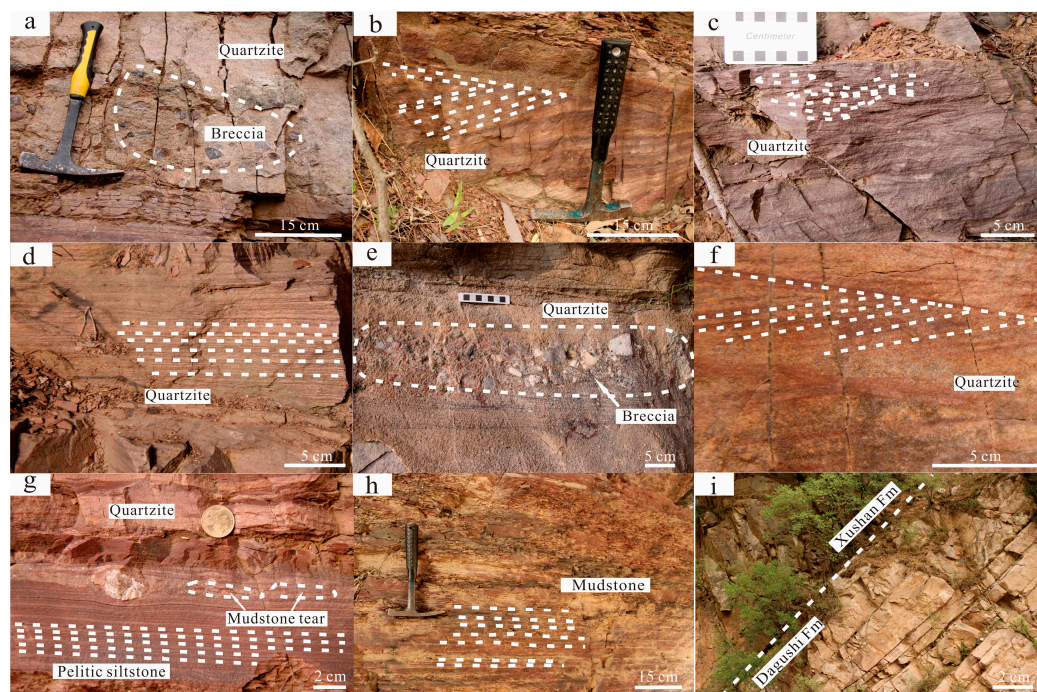


Figure 4. Lithologic characteristics and sedimentary structure of the Dagushi Formation in the Xiaogoubei section of Jiyuan. (a) Normal-grading bedding; (b) wedge-shaped cross-bedding; (c) trough cross-bedding; (d) parallel bedding; (e) conglomerate and trough cross-bedding; (f) wedge-shaped cross-bedding; (g) parallel bedding; (h) irregular horizontal bedding; (i) the boundary between the Dagushi and Xushan Formations.

4.2. Zircon U–Pb Geochronology

The CL images of representative zircons and their U–Pb ages are presented in Figures 5 and 6a,c. Most zircons are polyhedral in shape. Ref. [65] introduced that the calculation process of the age data. The analysis data are shown in Table S1, and the results show that the confidence intervals of zircon ranged from 90% to 100%. The ICP-MS U–Pb chronological test was performed on two sandstone samples collected from the top and bottom of the Dagushi Formation in the Huangbeijiao section of the Jiyuan area. The U–Pb age Concordia plot, age distribution histogram, and Th/U plot have the following characteristics (Figure 6):

Sample DGS-02 was collected from the bottom of the Dagushi Formation in Jiyuan (Figure 2). The age ranges of the 87 zircon grains were between 1784 and 2721 Ma. There were two main age peaks (1905 and 2154 Ma) and three secondary peaks (2295, 2536, and 2720 Ma) (Figure 6a,b). The youngest zircon U–Pb age measured from this sample was 1784 ± 43 Ma (concordant 99%). The Th/U value was between 0.31 and 1.40. Sample DGS-26 was collected from the top of the Dagushi Formation in Jiyuan (Figure 2). The age ranges of the 90 zircon grains were between 1832 and 2850 Ma, with three main peaks (2162, 2529, and 2713 Ma) and a secondary peak (1925 Ma) (Figure 6c,d). The youngest zircon U–Pb age measured from this sample was 1832 ± 34 Ma (concordant 99%). The Th/U value was between 0.07 and 1.22.

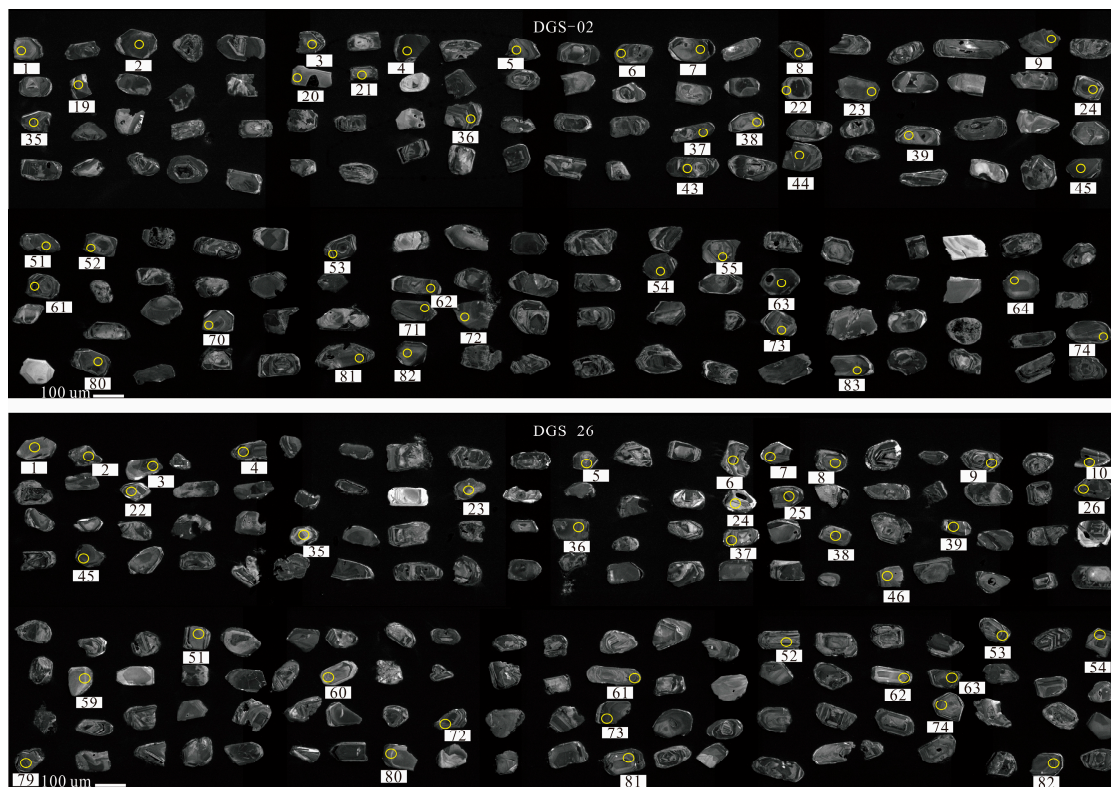


Figure 5. Cathodoluminescence (CL) images of representative zircons from the Dagushi Formation in Jiyuan (samples DGS-02 and DGS-26).

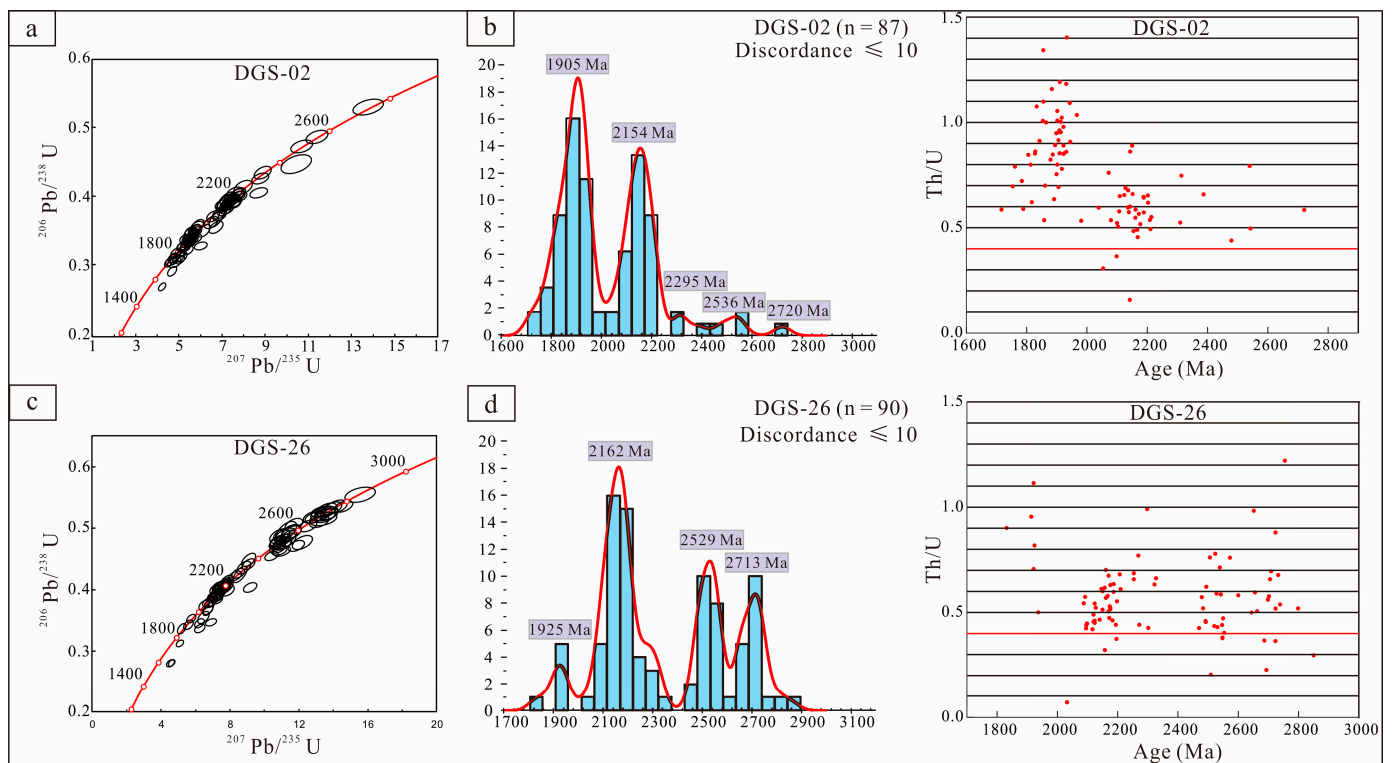


Figure 6. U-Pb age Concordia diagram, age distribution histogram, and Th/U age diagram of detrital zircons from the Dagushi Formation in Jiyuan; (a,b) DGS-02; (c,d) DGS-26.

4.3. Whole Rock Geochemistry

The major element compositions of the sandstones and trace element compositions of the argillaceous rocks are listed in Table S2. The sandstone samples from the Dagushi Formation were characterized by low SiO_2 contents (45.5%–77.9%), high $\text{Fe}_2\text{O}_3^{\text{T}} + \text{MgO}$ contents (2.7%–12.4%), and low TiO_2 contents (0.2%–0.8%). The Al_2O_3 and K_2O contents of the samples were 10.5%–20.4% and 1.7%–5.1%, respectively, while the MgO and Na_2O contents were 0.4%–4.1% and 0.2%–3.4%, respectively. We calculated the Chemical Index of Alteration (CIA) = $100 [\text{Al}_2\text{O}_3 / (\text{Al}_2\text{O}_3 + \text{CaO}^* + \text{Na}_2\text{O} + \text{K}_2\text{O})]$ (Table S2) [66], which yielded values for the sandstone samples from the Dagushi Formation that varied between 60.8 and 76.7 (average value: 66.4) and are indicative of a slightly to moderately weathered source [66–68] (Figure 7). We also calculated the Index of Compositional Variability (ICV) = $(\text{Fe}_2\text{O}_3 + \text{K}_2\text{O} + \text{Na}_2\text{O} + \text{CaO} + \text{MgO} + \text{TiO}_2) / \text{Al}_2\text{O}_3$ (Table S2) in order to determine the proportion of primary source material relative to the weathered minerals that occurred in the sedimentary rocks [69,70]. Calculated ICV values for the Dagushi Formation sandstones generally varied between 0.8 and 1.3 (average value: 1). The ICV values of these samples were greater than 1 or close to 1, which indicates the first cyclic sediments [70].

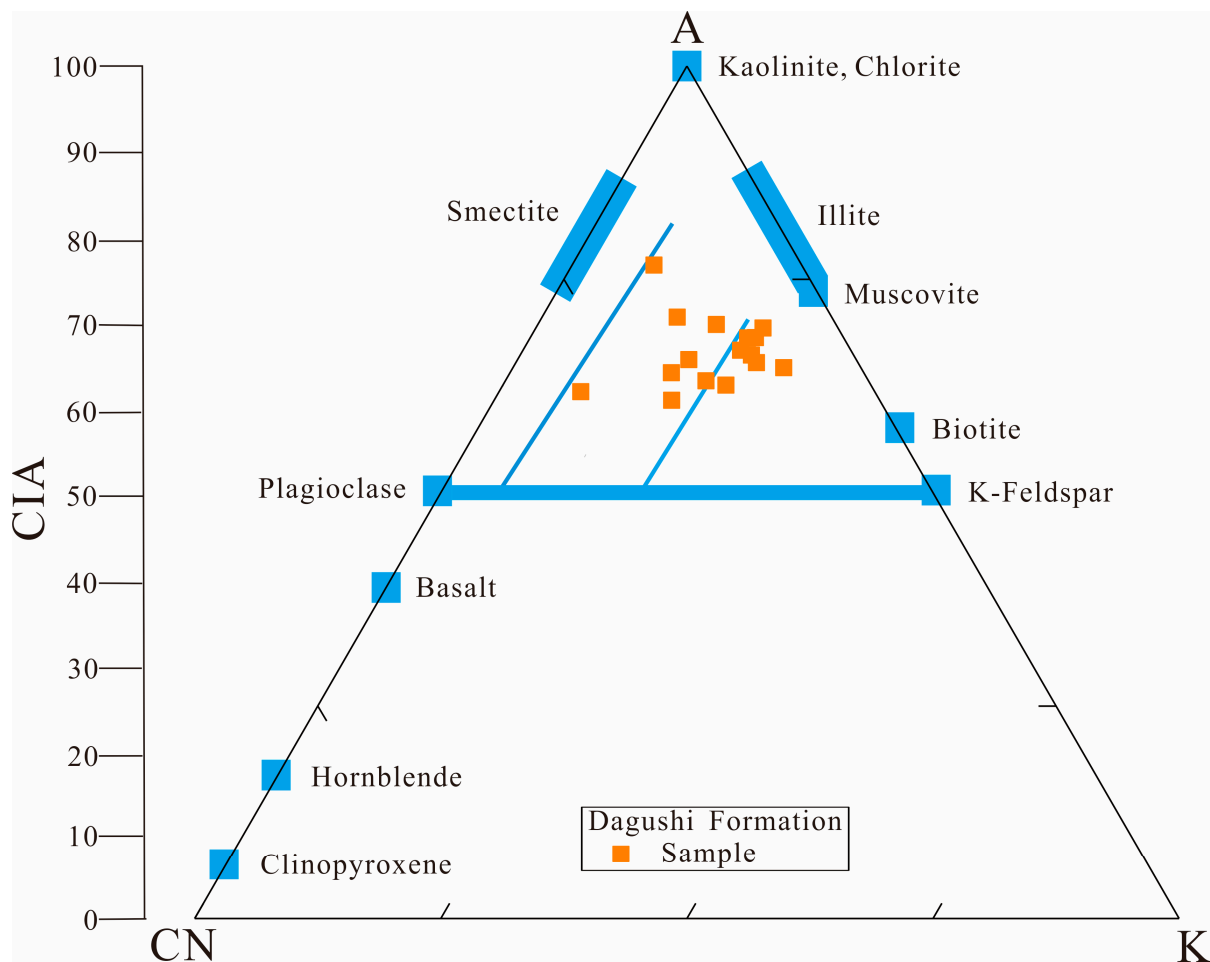


Figure 7. A–CN–K diagram of sandstones from the Dagushi Formation in Jiyuan (modified based on [66–68]). A = Al_2O_3 ; CN = $\text{CaO}^* + \text{Na}_2\text{O}$; K = K_2O ; CaO^* refers only to CaO in the silicate minerals, which is the molar coefficient of oxide.

The REE test results ($\times 10^{-6}$) and partial characteristic indices (Table S2) of the mudstones sample from the Dagushi Formation indicated that the total REE contents of the mudstones ranged between 185 and 368 $\mu\text{g/g}$ (average value: 258), which is greater than the averages for the North America shale (173 $\mu\text{g/g}$). Similarly, the $\Sigma\text{LREE}/\Sigma\text{HREE}$ values

varied from 9 to 13 (average value: 11), which is indicative of LREE enrichment. According to the chondrite-normalized REE patterns diagram [71] (Figure 8a), the La_N/Yb_N ratios ranged from 9.32 to 15.44, and the Gd_N/Yb_N ratios ranged from 1.52 to 1.89, indicating obvious fractionation of light and heavy REEs. δEu ranged from 0.56 to 0.74 (average value: 0.64), showing an obvious negative anomaly. δCe ranged from 0.99 to 1.12 (average value: 1.03), showing no obvious abnormality. Figure 8b shows that the La_A/Yb_A ratios ranged from 1.34 to 2.22 (average value: 1.84). LREEs were slightly enriched, and the overall content of REEs displayed a roughly synchronous change [72]. As shown in Figure 8c, the contents of the large ion lithophile elements Ba, Nb, and Sr were depleted, and Rb, Th, La, Ce, and Nd were enriched [71]. The contents of the transition elements, such as Ba, Rb, Y, Sc, V, Cr, Co, and Ni, were higher than the average values of the trace elements in the UCC, and the contents of terrigenous elements, such as Th, Zr, and Hf, were higher than their average values in the UCC [73] (Figure 8d).

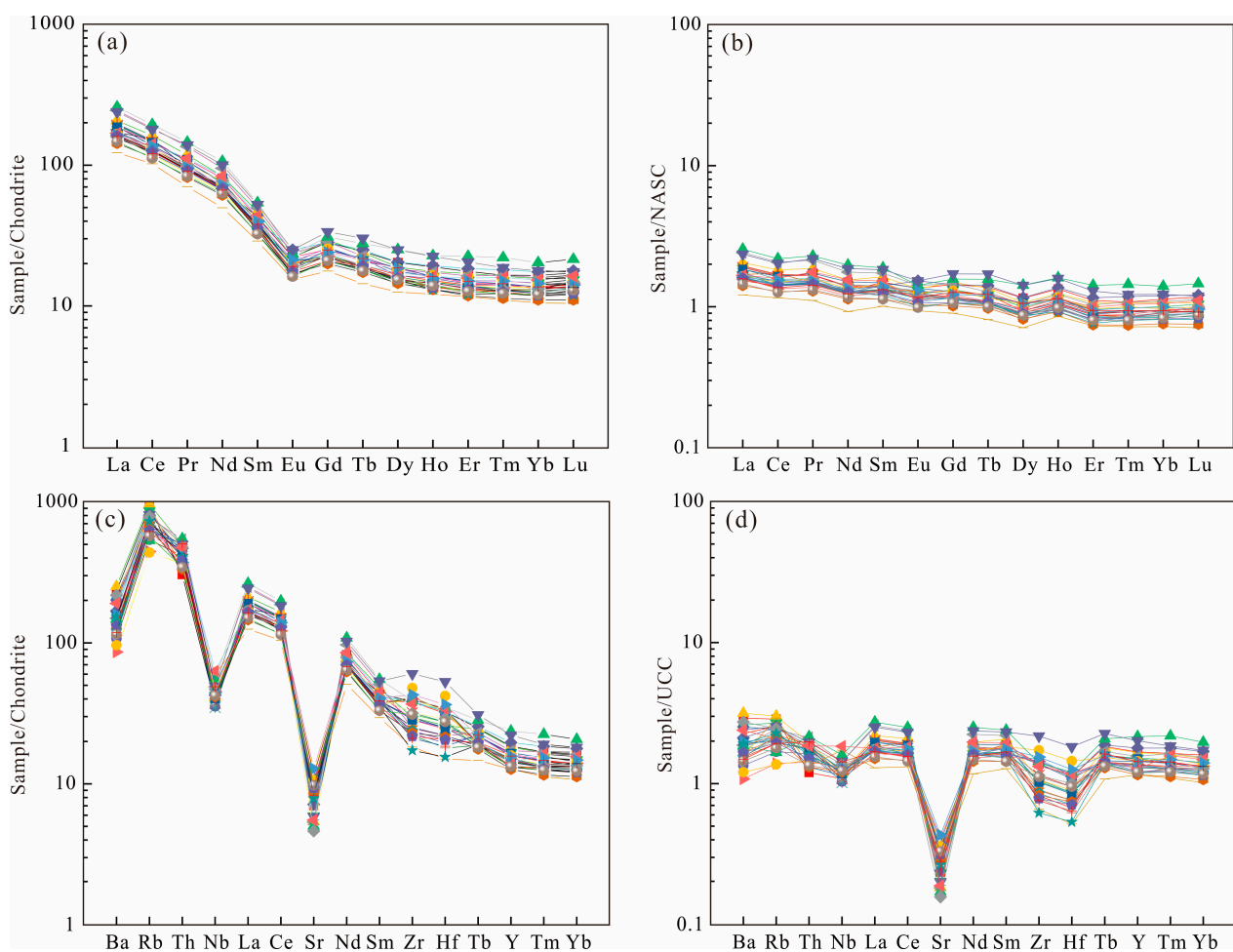


Figure 8. Distribution patterns of normalized rare earth elements (REEs) and normalized trace elements of argillaceous rock from the Mesoproterozoic Dagushi Formation in Jiyuan; (a,c) chondrite data from [71]; (b) North American shale (NASC) data from [72]; (d) UCC data from [73].

5. Discussion

5.1. Sedimentary Provenance of the Dagushi Formation

The results of the detrital zircon from the sandstone samples (DGS-02 and DGS-26) at the bottom of the Dagushi Formation in the Jiyuan area indicated that there were two primary age peaks, 1908 and 2147 Ma, and three secondary peaks, 2291, 2517, and 2713 Ma (Figure 9). This implied that the provenance was dominated by Paleoproterozoic geological bodies, with a small number of Neoproterozoic ones. The age peak at 2713 Ma corresponded

to the growth period of the Neoproterozoic crust [5,74–77]. In the Lushan area near Jiyuan, Trondhjemite, Tonalite, and Granodiorite (TTG) gneiss, plagioclase amphibolite, garnet two-pyroxene granulite, aluminum-rich and carbon-rich gneiss, marble, quartzite, etc. of the Taihua Group (2800–2700 Ma) were widely distributed [46,49,78] (Figure 9). The age peak at 2517 Ma corresponded to the tectonic–magmatic events of the late Neoproterozoic era, which was an important stage of continental crust accretion and cratonization in the NCC [79–83]. The detrital zircons between 2650 and 2500 Ma were likely derived from the TTG gneiss and supracrustal rock of the Dengfeng complex [5,42,84–89] (Figure 9). The age peaks of 2147 and 2291 Ma corresponded to multiple Paleoproterozoic active tectonic zones which developed during 2350–1950 Ma in the NCC; for example, the Shanxi–Henan active zone and the supracrustal rocks of the Songshan Group were formed between 2350–1960 Ma [28,51,90] (Figure 9). The age peak at 1908 Ma corresponded to tectonic–thermal events of collision and suturing between the eastern and western blocks of North China [2,4,91–95] (Figure 9). The ages of detrital zircons indicated that the provenance of the Dagushi Formation was primarily the NCC basement.

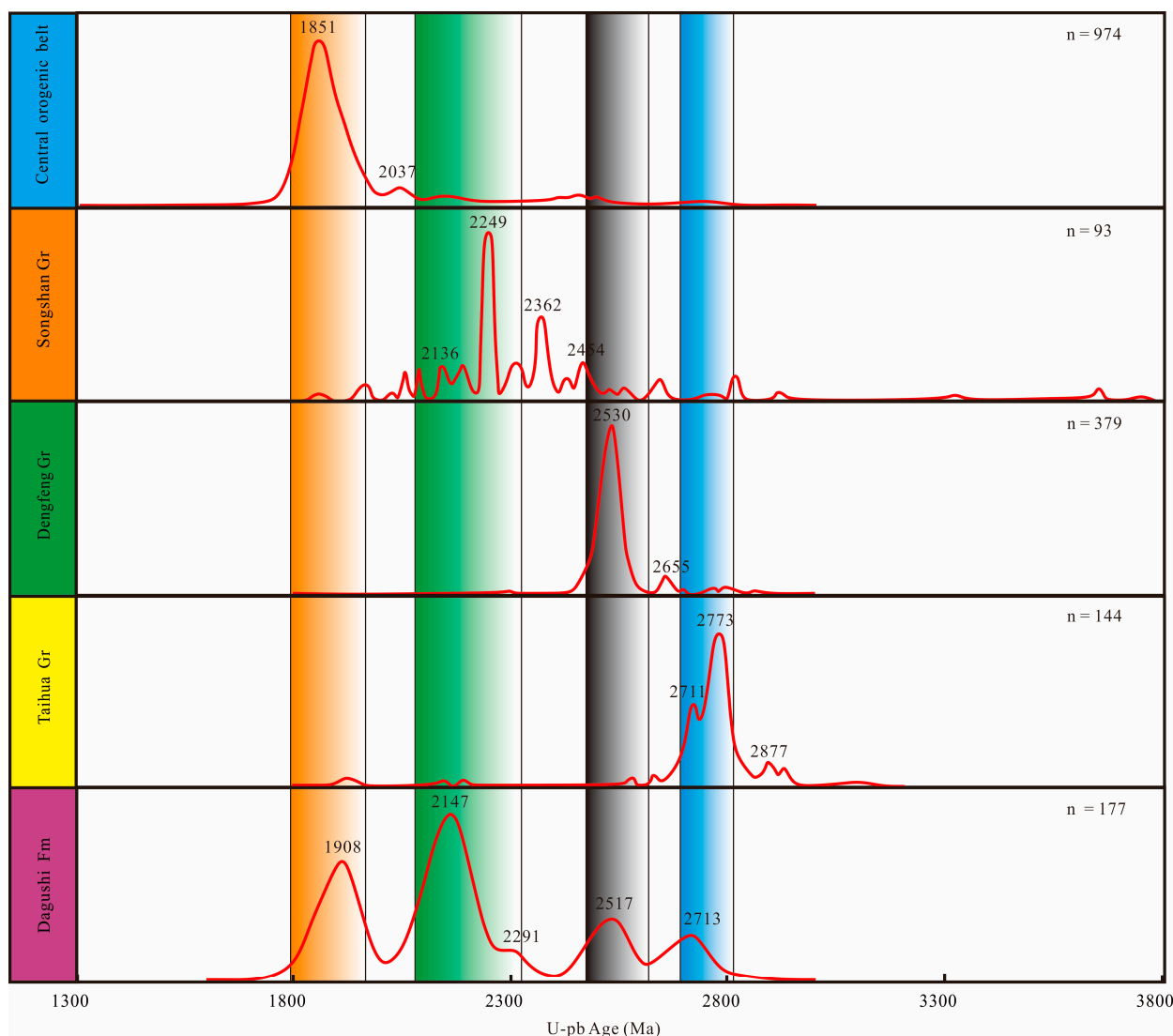


Figure 9. Histograms of concordant detrital zircon $^{207}\text{Pb}/^{206}\text{Pb}$ ages for samples from the Dagushi Formation, the Taihua, Dengfeng, and Songshan Groups, and the Central Orogenic Belt. Data sources: Dagushi Formation (this study); Taihua Group [46,49,78]; Dengfeng Group [86,88,89]; Songshan Group [90]; Central Orogenic Belt [2,4,91–95].

Based on the sandstone type discrimination diagram of $\log(\text{SiO}_2/\text{Al}_2\text{O}_3)$ - $\log(\text{Fe}_2\text{O}_3/\text{K}_2\text{O})$ [96], the sandstones of the Dagushi Formation were found to be low-maturity wacke, litharenite sublitharenite, and arkose (Figure 10), which indicated that these sandstones in the Jiyuan area had undergone rapid proximal accumulation.

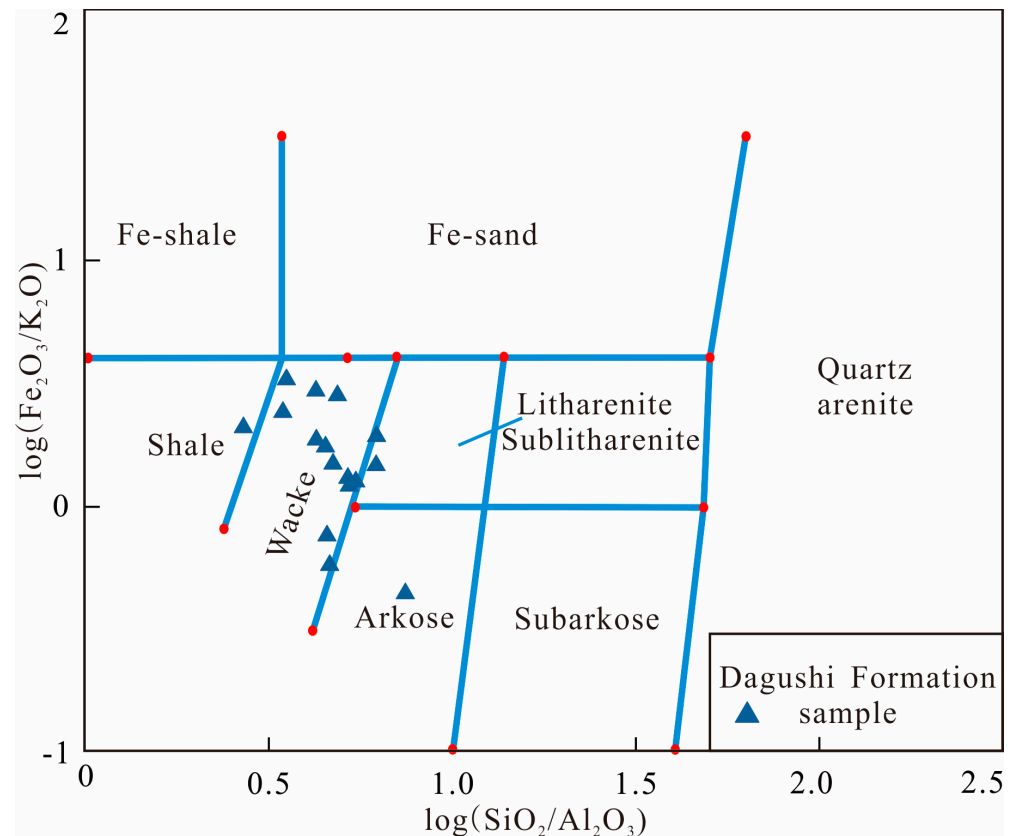


Figure 10. Discrimination plot of sandstone type for the Mesoproterozoic Dagushi Formation in Jiyuan (modified after [96]).

Several trace elements and REEs of clastic sedimentary rocks were inherited from their parent rocks and have been used to show their properties [97–100]. The discrimination diagram of the argillaceous rock of $\text{La}/\text{Yb}-\text{Ce}$ [101] (Figure 11a) shows that the distribution of argillaceous rocks from the Dagushi Formation form a cluster located in the field for intermediate and silicate rocks. The diagram of $\text{La}/\text{Sc}-\text{Co}/\text{Th}$ [101] (Figure 11b) shows that the argillaceous rock samples from the Dagushi Formation plot near felsic volcanic rocks. The $\text{La}/\text{Yb}-\sum\text{REE}$ discrimination diagram of the source rock [102] (Figure 11c) reveals that the scatter plot distribution of argillaceous rocks in the Dagushi Formation was concentrated in the granite field. The discrimination diagram of $\text{La}/\text{Th}-\text{Hf}$ [103] (Figure 11d) shows that the argillaceous rock samples of the Dagushi Formation were located near the felsic provenance area, with only a few in the passive continental provenance and mixed provenance areas of felsic and mafic rocks. The discrimination diagram of $\text{Zr}/\text{Sc}-\text{Th}/\text{Sc}$ [104] (Figure 11e) shows that the projective points of argillaceous rock samples from the Dagushi Formation fell near the upper crust (felsic volcanic rocks). Based on regional geological data, the felsic metamorphic crystalline basement and granitic rocks in the late Archean–Paleoproterozoic era were widely distributed in the Wangwu Mountain area where Jiyuan is located [24,25,105,106]. For this reason, the sources of argillaceous rocks from the Dagushi Formation were primarily felsic in provenance. The provenance area pointed to is the underlying metamorphic crystalline basement of the NCC.

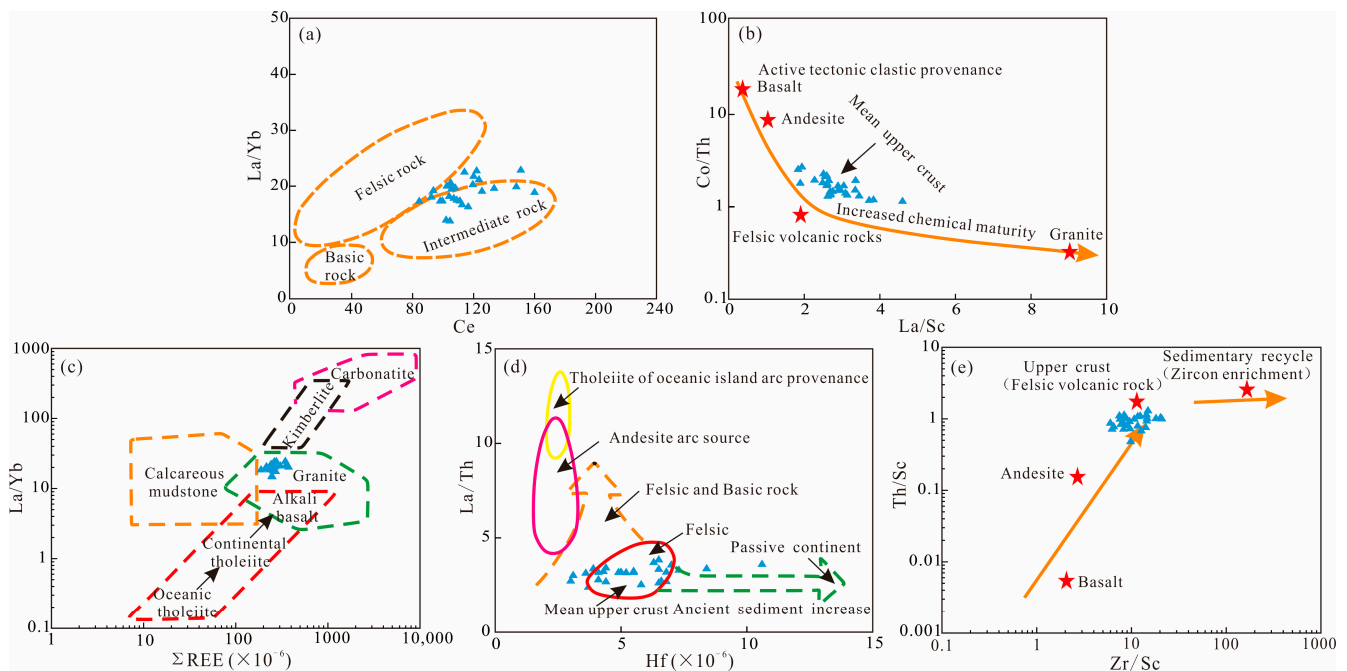


Figure 11. Source discrimination diagrams of argillaceous rock from the Mesoproterozoic Dagushi Formation in Jiyuan; (a,b) modified after [101]; (c) modified after [102]; (d) modified after [103]; (e) modified after [104].

The diagrams of trace elements Th–Sc–Zr/10 and Th–Co–Zr/10 (Figure 12a,b) and major elements $\text{wt}(\text{Fe}_2\text{O}_3^{\text{T}} + \text{MgO})\% - \text{wt}(\text{TiO}_2)\%$ and $\text{wt}(\text{Fe}_2\text{O}_3^{\text{T}} + \text{MgO})\% - \text{wt}(\text{Al}_2\text{O}_3)\% / \text{wt}(\text{SiO}_2)\%$ (Figure 12c,d) have been used to distinguish tectonic environments [98,107–112]. Based on the discrimination diagrams of Th–Sc–Zr/10 and Th–Co–Zr/10 (Figure 12a,b), the argillaceous rock sample from the Dagushi Formation in the Jiyuan area primarily fell into the continent island arc and active continental margin, with a few samples in the nearby area. Based on discrimination diagrams of $\text{wt}(\text{Fe}_2\text{O}_3^{\text{T}} + \text{MgO})\% - \text{wt}(\text{TiO}_2)\%$ (Figure 12c), the sandstone samples from the Dagushi Formation in the Jiyuan area also primarily fell into the continent island arc and active continental margin fields, with a few near the ocean island arc field. The discrimination diagrams of $\text{wt}(\text{Fe}_2\text{O}_3^{\text{T}} + \text{MgO})\% - \text{wt}(\text{Al}_2\text{O}_3)\% / \text{wt}(\text{SiO}_2)\%$ (Figure 12d) show that most samples fell into the active continental margin, ocean island arc field, and nearby areas, with a few in the ocean island arc field. Thus, the above findings indicated that the provenance area showed mixed provenance characteristics dominated by the active tectonic setting, supplemented by the settings of an active continental margin and island arc. The tectonic settings identified above only reflected that of the provenance area and did not represent the tectonic settings for the formation of the Dagushi Formation. The determination of the tectonic background during the sedimentary period of the Dagushi Formation in the Xionger Group should refer to evidence of coeval magmatic rocks in the Xionger Group. However, judgment of the tectonic background of the Dagushi Formation and even the Xionger Group is still controversial. To date, the main viewpoints include an Andean-type continental margin [9,22], passive continental margin and rift [26–28,36,37], and active continental margin and rift [22]. Thus far, the above viewpoints have not been unified to reach consensus.

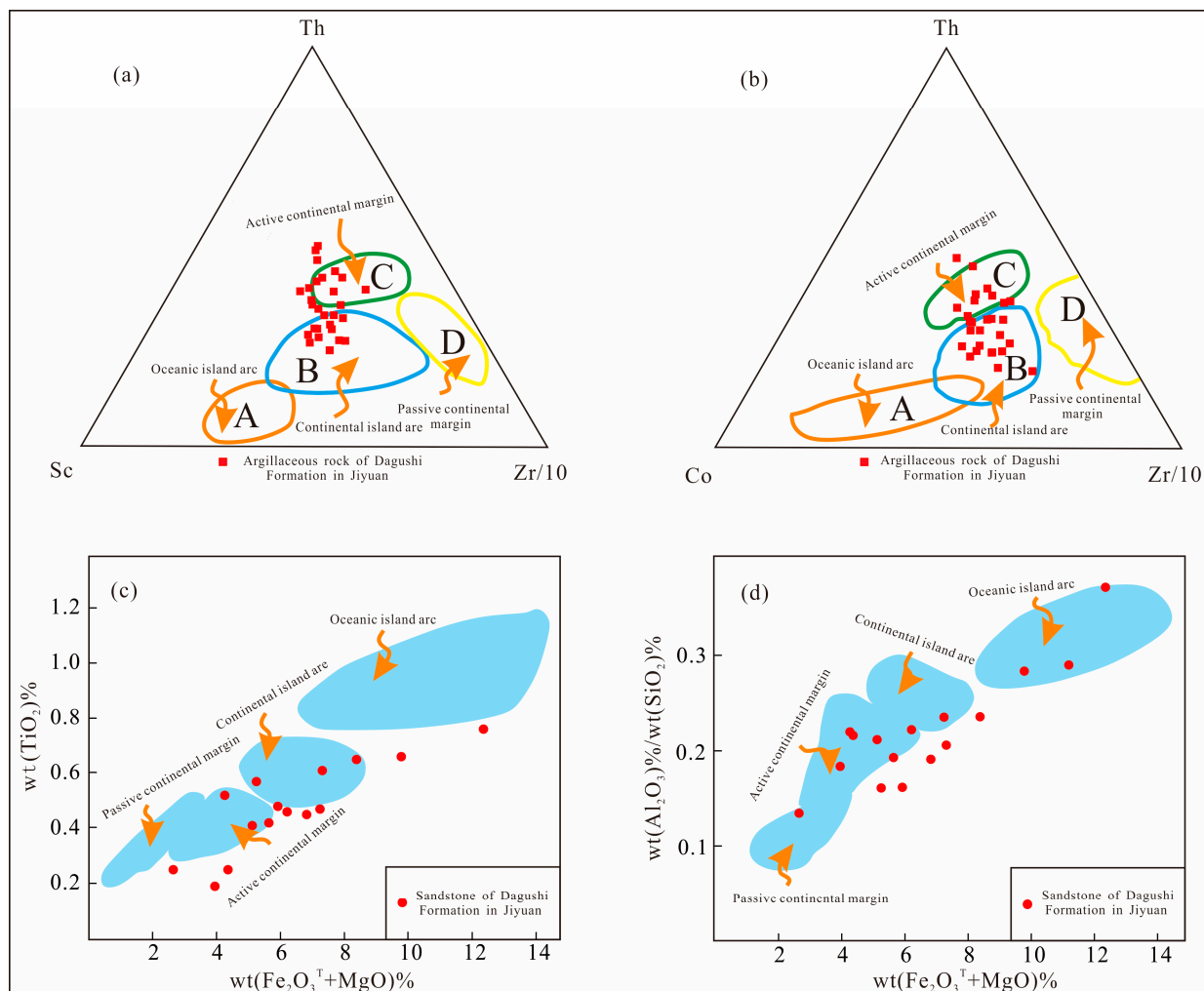


Figure 12. Discrimination plot of tectonic background for sandstone and argillaceous source rocks from the Mesoproterozoic Dagushi Formation in Jiyuan; (a,b) modified after [107]; (c,d) modified after [108]. (a) Oceanic island arc; (b) Continental island arc; (c) Active continental margin; (d) Passive continental margin.

5.2. Tectonic and Sedimentary Implications of Dagushi Formation for the Southern NCC during the Mesoproterozoic

The North China Craton underwent multiple periods of continuous rift development from ~18 Ga to the Neoproterozoic. Among them, the Xiong'er Rift, located at the southern margin of the North China Craton, represents a significant continental stretching and fracturing event that developed in response to the rifting process of the Mesoproterozoic Columbia supercontinent within the context of extensional tectonics. During this rifting process, subsidence initially occurred in the regions of Yuanqu County—Jiyuan City, Luoning City—Luanchuan County, and Ruzhou City, located at the southern margin of the North China Craton (Figure 13a). Because of the difference in terrain elevation, the felsic crystalline basement of the relatively uplifted NCC was denuded quickly, and the product of basement denudation carried by rivers was removed from the basin margin and deposited in the adjacent depression. The coarse clastic sediments at the bottom were gradually superimposed and extended to the rift center, forming a set of clastic sedimentary strata consisting of coarse clastic sandstone and argillaceous clastic rock, i.e., the Dagushi Formation of the Xiong'er Group (Figure 13a). This was followed by large-scale and continuous volcanism throughout the entire region, resulting in the formation of the giant thick volcanic rocks of the Xiong'er Group. The clastic rock filling of the Dagushi Formation

in the Xiong'er Rift Basin and the subsequent eruption of the Xiong'er Group volcanic rocks originated from the tectonic setting of a continental margin rift [25,38,105,106] and represented the beginning of multi-stage fracturing events in the NCC from the end of the Paleoproterozoic era to the beginning of the Mesoproterozoic era, which was likely related to the transition of the Columbia supercontinent from collage and aggregation to stretching and fracturing.

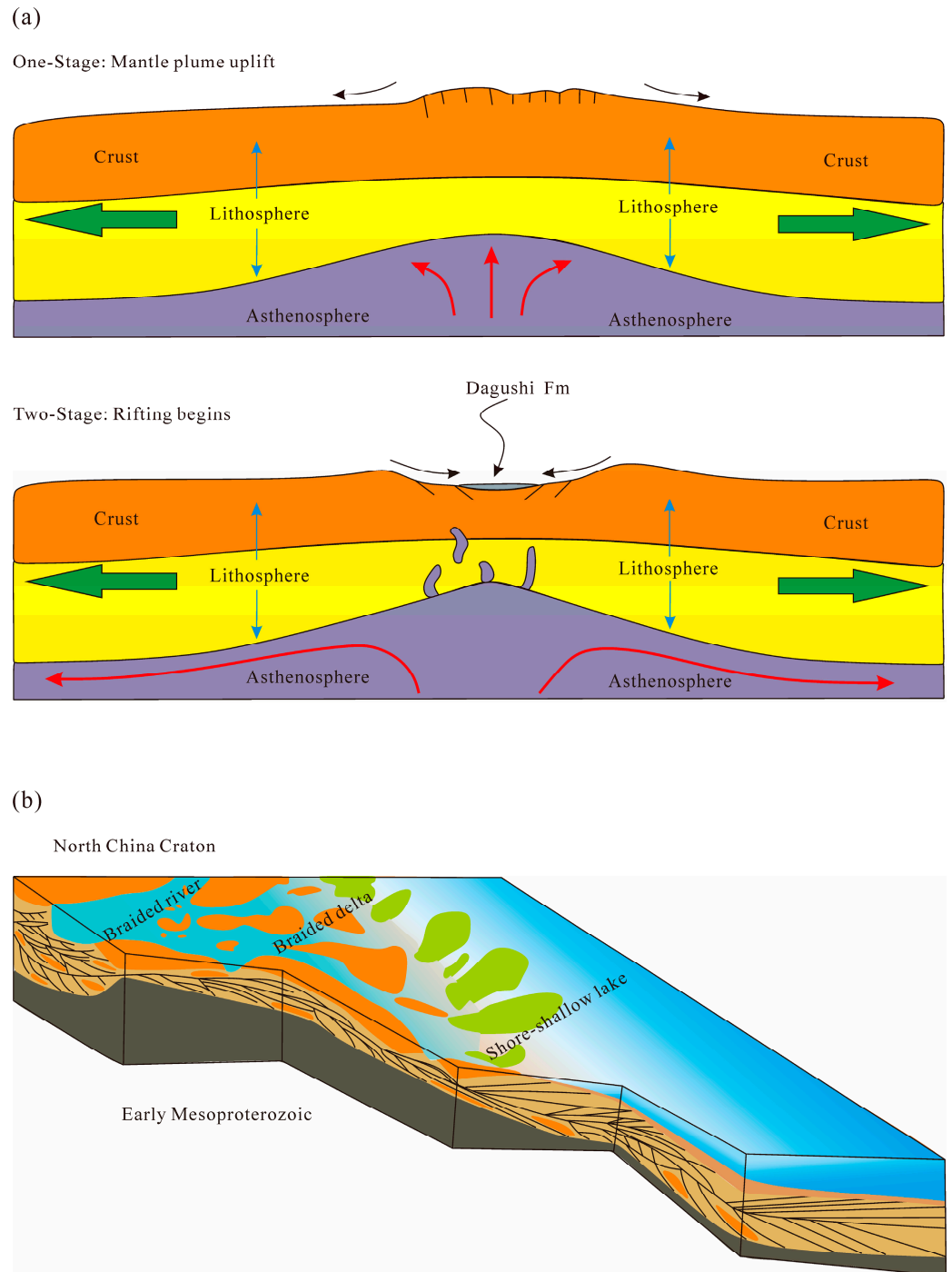


Figure 13. (a) Schematic section showing the location of our study area and the Dagushi Formation relative to tectonic units that might be provenance sources. (b) Proposed depositional model for the Dagushi Formation.

During the rapid sedimentary process of the Dagushi Formation in Jiyuan City, the initial stage was characterized by braided river facies, which resulted in the formation of sedimentary sandstones. As hydrodynamic conditions gradually weakened, the water body became deeper, leading to the development of delta facies with sand–mud interaction layers. This subsequently transformed upward into mudstone-based lake facies, and this vertical change marked the beginning of crustal fracturing and continuous sinking (Figure 13b). The Dagushi Formation, located at the base of the Xiong'er Group, is overlain by the unconformable Gaoshanhe Formation and Xiaogoubei Formation that consist of conglomerate and mixed sandstone. These sediments indicate several regional tectonic movements that occurred on the southern edge of North China before and after the eruption of the Xiong'er Volcano. Meanwhile, the Dagushi Formation represents the first regional subsidence since the Paleozoic era and distinguishes between the metamorphic basement of the Lower Paleoproterozoic Shuangfang Formation complex and the upper non-metamorphic Mesoproterozoic Xiong'er Group. It serves as a marker to delineate the earliest, non-metamorphic stable sedimentary cover on the crystalline basement of the North China Craton, which actually indicates the Paleoproterozoic and Mesoproterozoic boundary. The age of this study boundary is ~17.84 Ga, which is ~1.84 Ga earlier than the internationally recognized Paleoproterozoic and Mesoproterozoic boundary age.

6. Conclusions

By identifying the lithologic characteristics and sedimentary tectonics of the Dagushi Formation in the field, we determined that from bottom to top, the sedimentary facies of the Dagushi Formation are braided river, braid delta, and lake.

The CIA indicates a slightly to moderately weathered source, and ICV indicates the first cyclic sediments. The U–Pb ages of the detrital zircons of the Dagushi Formation indicate that the sediments were likely supplied by the Taihua, Dengfeng, and Songshan Groups and the Central Orogenic Belt.

The vertical facies and provenance changes of the Dagushi Formation reflect a continuous crust fracturing process that occurred in the North China Craton.

Supplementary Materials: The following supporting information can be downloaded at: <https://www.mdpi.com/article/10.3390/min13070971/s1>, Table S1: The ICP-MS U-Pb test data was performed on two sandstone samples collected from the DGS-02 and DGS-026 of the Dagushi Formation in the Jiyuan area; Table S2: For the major element assemblage of sandstone and trace element assemblage of argillaceous rock of Dagushi Formation in North China Craton.

Author Contributions: Conceptualization, Y.Z. and G.Z.; methodology, Y.Z.; software, Y.Z.; validation, Y.Z., G.Z. and F.S.; formal analysis, Y.Z.; investigation, Y.Z. and G.Z.; resources, Y.Z.; data curation, Y.Z.; writing—original draft preparation, Y.Z.; writing—review and editing, Y.Z.; visualization, Y.Z.; supervision, G.Z.; project administration, Y.Z. and F.S.; funding acquisition, Y.Z. and F.S. All authors have read and agreed to the published version of the manuscript.

Funding: This research was funded by the National Natural Science Foundation (grant no. 41872238). The APC was funded by Yuan Zhang.

Data Availability Statement: Not applicable.

Acknowledgments: Discussions with Deshun Zheng, Fengbo Sun, and Sicong Liu greatly improved the manuscript.

Conflicts of Interest: The authors declare no potential conflict of interest.

References

1. Chen, Y.J.; Zhai, M.G.; Jiang, S.Y. Significant achievements and open issues in study of orogeneses and metallogenesis surrounding the North China continent. *Acta Petrol. Sin.* **2009**, *25*, 2695–2726. (In Chinese with English abstract).
2. Zhao, G.C.; Wilde, S.A.; Guo, J.H.; Cawood, P.A.; Sun, M.; Li, X.P. Single zircon grains record two Paleoproterozoic collisional events in the North China Craton. *Precambrian Res.* **2010**, *177*, 266–276. [[CrossRef](#)]
3. Zhao, G.C.; Cawood, P.A. Precambrian geology of China. *Precambrian Res.* **2012**, *222*, 13–54. [[CrossRef](#)]

4. Zhao, G.C.; Zhai, M.G. Lithotectonic elements of Precambrian basement in the North China Craton: Review and tectonic implications. *Gondwana Res.* **2013**, *23*, 1207–1240. [[CrossRef](#)]
5. Zhai, M.G.; Santosh, M. The early Precambrian odyssey of the North China Craton: A synoptic overview. *Gondwana Res.* **2011**, *20*, 6–25. [[CrossRef](#)]
6. Zhai, M.G.; Zhao, Y.; Zhao, T.P. *Main Tectonic Events and Metallogeny of the North China Craton*; Springer: Singapore, 2016.
7. Kusky, T.M.; Li, J.H. Paleoproterozoic tectonic evolution of the North China Craton. *J. Asian Earth Sci.* **2003**, *22*, 383–397. [[CrossRef](#)]
8. Santosh, M.; Maruyama, S.; Yamamoto, S. The making and breaking of super-continents: Some speculations based on superplumes, super downwelling and the role of tectosphere. *Gondwana Res.* **2009**, *15*, 324–341. [[CrossRef](#)]
9. Zhao, G.C.; He, Y.H.; Sun, M. The Xiong'er volcanic belt at the southern margin of the North China Craton: Petrographic and geochemical evidence for its outboard position in the Paleo-Mesoproterozoic Columbia Supercontinent. *Gondwana Res.* **2009**, *16*, 170–181. [[CrossRef](#)]
10. Yang, Q.Y.; Santosh, M.; Rajesh, H.M.; Tsunogae, T. Late paleoproterozoic chamockite suite within post-collisional setting from the North China Craton: Petrology, geochemistry, zircon U-Pb geochronology and Lu-Hf isotopes. *Lithos* **2014**, *208*, 34–52. [[CrossRef](#)]
11. Zhao, G.C.; Wilde, S.A.; Cawood, P.A.; Sun, M. Thermal evolution of the Archaean basement rocks from the eastern part of the North China Craton and its bearing on tectonic setting. *Int. Geol. Rev.* **1998**, *40*, 706–721. [[CrossRef](#)]
12. Zhao, G.C.; Wilde, S.A.; Cawood, P.A.; Sun, M. Archaean blocks and their boundaries in the North China Craton: Lithological, geochemical, structural and P-T path constraints and tectonic evolution. *Precambrian Res.* **2001**, *107*, 45–73. [[CrossRef](#)]
13. Zhao, G.C.; Sun, M.; Wilde, S.A.; Li, S.Z. Assembly, accretion and break up of the Paleo-Mesoproterozoic Columbia supercontinent: Records in the North China Craton. *Gondwana Res.* **2003**, *6*, 417–434. [[CrossRef](#)]
14. Zhao, G.C.; Kroner, A.; Wilde, S.A.; Sun, M.; Li, S.Z.; Li, X.P.; Zhang, J.; Xia, X.P.; He, Y.H. Lithotectonic elements and geological events in the Hengshan-Wutai-Fuping belt: A synthesis and implications for the evolution of the Trans-North China Orogen. *Geol. Mag.* **2007**, *144*, 753–775. [[CrossRef](#)]
15. Rogers, J.J.W.; Santosh, M. Configuration of Columbia, a Mesoproterozoic supercontinent. *Gondwana Res.* **2002**, *5*, 5–22. [[CrossRef](#)]
16. Zhao, G.C.; Cawood, P.A.; Wilde, S.A.; Sun, M. Review of global 2.1–1.8 Ga orogens: Implications for a pre-Rodinia supercontinent. *Earth-Sci. Rev.* **2002**, *59*, 125–162. [[CrossRef](#)]
17. Zhao, G.C.; Sun, M.; Wilde, S.A.; Li, S.Z. A Paleo-Mesoproterozoic supercontinent: Assembly, growth and breakup. *Earth-Sci. Rev.* **2004**, *67*, 91–123. [[CrossRef](#)]
18. He, Y.H.; Zhao, G.Z.; Sun, M.; Wilde, S.A. Geochemistry, isotope systematics and petrogenesis of the volcanic rocks in the Zhongtiao Mountain: An alternative interpretation for the evolution of the southern margin of the North China Craton. *Lithos* **2008**, *102*, 157–178. [[CrossRef](#)]
19. Peng, P.; Zhai, M.G.; Ernst, R.E.; Guo, J.H.; Liu, F.; Hu, B. A 1.78 Ga large igneous province in the North China craton: The Xiong'er volcanic province and the North China dyke Swarm. *Lithos* **2008**, *101*, 260–280. [[CrossRef](#)]
20. Geng, Y.S.; Kuang, H.W.; Du, L.L.; Liu, Y.Q.; Zhao, T.P. On the Paleo-Mesoproterozoic boundary from the breakup event of the Columbia supercontinent. *Acta Petrol. Sin.* **2019**, *35*, 2299–2324.
21. Sun, S.; Zhang, G.W.; Chen, Z.M. *Precambrian Geological Evolution in the South of North China Fault Block*; Metallurgical Industry Press: Beijing, China, 1985. (In Chinese)
22. Chen, Y.J.; Fu, S.G.; Qiang, L.Z. The Tectonic environment for the formation of the Xiong'er Group and the Xiyanghe Group. *Geol. Rev.* **1992**, *38*, 325–333. (In Chinese with English abstract).
23. Zhao, T.P.; Zhou, M.F.; Jin, C.W.; Guan, H.; Li, H.M. Discussion on age of the Xiong'er Group in southern margin of North China Craton. *Sci. Geol.-Gica. Sin.* **2001**, *36*, 326–334. (In Chinese with English abstract).
24. Zhao, T.P.; Zhai, M.G.; Xia, B.; Li, H.M.; Zhang, Y.X.; Wan, Y.S. Zircon U-Pb SHRIMP dating for the volcanic rocks of the Xiong'er Group: Constrains on the initial formation age of the cover of the North China Craton. *Chinese Sci. Bull.* **2004**, *49*, 2495–2502. [[CrossRef](#)]
25. Zhao, T.P.; Xu, Y.H.; Zhai, M.G. Petrogenesis and Tectonic Setting of the Paleoproterozoic Xiong'er Group in the Southern Part of the North China Craton: A Review. *Geol. J. China Univ.* **2007**, *13*, 191–206. (In Chinese with English abstract).
26. Zhai, M.G. 2.1–1.7 Ga geological event group and its geotectonic significance. *Acta Petrol. Sin.* **2004**, *20*, 1343–1354. (In Chinese with English abstract).
27. Zhai, M.G. Multi-stage crustal growth and cratonization of the North China Craton. *Geosci. Front.* **2014**, *5*, 457–469. [[CrossRef](#)]
28. Zhai, M.G.; Peng, P. Paleoproterozoic events in North China Craton. *Acta Petrol. Sin.* **2007**, *23*, 2665–2682. (In Chinese with English abstract).
29. Kusky, T.; Li, J.G.; Santosh, M. The Paleoproterozoic North Hebei orogen: North China craton's collisional suture with the Columbia supercontinent. *Gondwana Res. Int. Geosci. J.* **2007**, *12*, 4–28. [[CrossRef](#)]
30. He, Y.H.; Zhao, G.C.; Sun, M.; Xia, X.P. SHRIMP and LA-ICP-MS zircon geochronology of the Xiong'er volcanic rocks: Implications for the Paleo-Mesoproterozoic evolution of the southern margin of the North China Craton. *Precambrian Res.* **2009**, *168*, 213–222. [[CrossRef](#)]
31. He, Y.H.; Zhao, G.C.; Sun, M.; Han, Y.G. Petrogenesis and tectonic setting of volcanic rocks in the Xiaoshan and Waifangshan areas along the southern margin of the North China Craton: Constraints from bulk-rock geochemistry and Sr-Nd isotopic composition. *Lithos* **2010**, *114*, 186–199. [[CrossRef](#)]

32. Hu, G.H.; Zhao, T.P.; Zhou, Y.Y.; Yang, Y. Depositional age and provenance of the Wufoshan Group in the southern margin of the North China Craton: Evidence from detrital zircon U-Pb ages and Hf isotopic compositions. *Geochimica* **2012**, *41*, 326–342, (in Chinese with English abstract).
33. Hu, G.H.; Zhou, Y.Y.; Zhao, T.P. Geochemistry of Proterozoic Wufoshan Group sedimentary rocks in the Songshan area, Henan Province: Implications for provenance and tectonic setting. *Acta Petrol. Sin.* **2012**, *28*, 3692–3704, (In Chinese with English abstract).
34. Hu, G.H.; Zhao, T.P.; Zhou, Y.Y.; Wang, S.Y. Meso-Neoproterozoic sedimentary formation in the southern margin of the North China Craton and its geological implications. *Acta Petrol. Sin.* **2013**, *29*, 2491–2507, (In Chinese with English abstract).
35. Hu, G.H.; Zhao, T.P.; Zhou, Y.Y. Depositional age, provenance and tectonic setting of the Proterozoic Ruyang Group, southern margin of the North China Craton. *Precambrian Res.* **2014**, *246*, 296–318. [[CrossRef](#)]
36. Zhai, M.G. Where is the north China-South China block boundary in eastern China? Comment. *Geology* **2002**, *30*, 667, (In Chinese with English abstract).
37. Zhai, M.G.; Hu, B.; Zhao, T.P.; Peng, P.; Meng, Q.R. Late Paleoproterozoic-Neoproterozoic multi-rifting events in the North China Craton and their geological significance: A study advance and review. *Tectonophysics* **2015**, *662*, 153–166. [[CrossRef](#)]
38. Xu, Y.H.; Zhao, T.P.; Zhang, Y.X.; Chen, W. Geochemical Characteristics and Geological Significances of the Dagushi Formation Siliciclastic Rocks, the Paleoproterozoic Xiong'er Group from the Southern North China Craton. *Geol. Rev.* **2008**, *54*, 316–326, (in Chinese with English abstract).
39. Xu, Y.H.; Zhao, T.P.; Chen, W. The Discovery and Geological Significance of Glauconites from the Palaeoproterozoic Xiong'er Group in the Southern Part of the North China Craton. *Acta Sedimentol. Sin.* **2010**, *28*, 671–675, (In Chinese with English abstract).
40. Deng, H.; Kusky, T.M.; Polat, A.L.; Fu, H.Q.; Wang, L.; Wang, J.P.; Wang, S.J.; Zhai, W.J. A Neoproterozoic arc-backarc pair in the Linshan Massif, southern North China Craton. *Precambrian Res.* **2020**, *341*, 105649. [[CrossRef](#)]
41. Henan Bureau of Geology and Mineral Resources. *Regional Geology of Henan Province*; Geological Publishing House: Beijing, China, 1989. (In Chinese)
42. Zhai, M.G.; Guo, J.H.; Liu, W.J. Neoproterozoic to Paleoproterozoic continental evolution and tectonic history of the North China Craton. *J. Asian Earth Sci.* **2005**, *24*, 547–561. [[CrossRef](#)]
43. Zhao, G.C.; Sun, M.; Wilde, S.A.; Li, S.Z. Late Archean to Paleoproterozoic evolution of the North China Craton: Key issues revisited. *Precambrian Res.* **2005**, *136*, 177–202. [[CrossRef](#)]
44. Jahn, B.M. Early crustal evolution as viewed from Archean basic rocks of China. *Chem. Geol.* **1988**, *70*, 141. [[CrossRef](#)]
45. O'Neill, C.; Lenardic, A.; Moresi, L.; Torsvik, T.H.; Lee, C.T.A. Episodic Precambrian subduction. *Earth Planet. Sci. Lett.* **2007**, *262*, 552–562. [[CrossRef](#)]
46. Huang, X.L.; Niu, Y.L.; Xu, Y.G.; Yang, Q.J.; Zhong, J.W. Geochemistry of TTG and TTG-like gneisses from Lushan-Taihua complex in the southern North China Craton: Implications for late Archean crustal accretion. *Precambrian Res.* **2010**, *182*, 43–56. [[CrossRef](#)]
47. Wan, Y.S.; Dong, C.Y.; Wang, W.; Xie, H.Q.; Liu, D.Y. Archean Basement and a Paleoproterozoic Collision Orogen in the Huoqiu Area at the Southeastern Margin of North China Craton: Evidence from Sensitive High Resolution Ion Micro-Probe U-Pb Zircon Geochronology. *Acta Geol. Sin.-Engl. Ed.* **2010**, *84*, 91–104. [[CrossRef](#)]
48. Wan, Y.S.; Liu, D.Y.; Wang, S.J.; Yang, E.X.; Wang, W.; Dong, C.Y.; Zhou, H.Y.; Du, L.L.; Yang, Y.H.; Diwu, C.R. ~2.7 Ga juvenile crust formation in the North China Craton (Taishan-Xintai area, western Shandong Province): Further evidence of an understated event from U-Pb dating and Hf isotopic composition of zircon. *Precambrian Res.* **2011**, *186*, 169–180. [[CrossRef](#)]
49. Diwu, C.R.; Sun, Y.; Lin, C.L.; Wang, H.L. LA-(MC)-ICPMS U-Pb zircon geochronology and Lu-Hf isotope compositions of the Taihua Complex on the southern margin of the North China Craton. *Chin. Sci. Bull.* **2010**, *55*, 2112–2123, (In Chinese with English abstract). [[CrossRef](#)]
50. Zhai, M.G.; Bian, A.G.; Zhao, T.P. The amalgamation of the supercontinent of North China Craton at the end of Neo-Archaean and its breakup during late Palaeoproterozoic and Meso-Proterozoic. *Sci. China (Series D)* **2000**, *43*, 219–232. [[CrossRef](#)]
51. Zhai, M.G.; Liu, W. Palaeoproterozoic tectonic history of the North China Craton: A review. *Precambrian Res.* **2003**, *122*, 183–199. [[CrossRef](#)]
52. Zhao, T.P.; Zhou, M.F.; Zhai, M.G.; Xia, B. Palaeoproterozoic rift-related volcanism of the Xiong'er Group in the North China Craton: implications for the breakup of Columbia. *Int. Geol. Rev.* **2002**, *44*, 336–351. [[CrossRef](#)]
53. Guan, B.D. *The Precambrian-Lower Cambrian Geology and Metallogenesis in the South Border of the North China Platform in Henan Province*; Press of China University of Geosciences: Wuhan, China, 1996; pp. 1–328. (In Chinese)
54. Zhao, T.P.; Yuan, Z.L.; Guan, B.D. The characteristics and sedimentary environment of sedimentary interbeds of Xiong'er Group distributed in the juncture of Henan-Shanxi-Shaanxi Provinces. *Henan Geol.* **1998**, *16*, 261–272, (In Chinese with English abstract).
55. Nasdala, L.; Hofmeister, W.; Norberg, N.; Martinson, J.M.; Corfu, F.; Dörr, W.; Kamo, S.L.; Kennedy, A.K.; Kronz, A.; Reiners, P.W.; et al. Zircon M257: A homogeneous natural reference material for the ion microprobe U-Pb analysis of zircon. *Geostand. Geoanal. Res.* **2008**, *32*, 247–265. [[CrossRef](#)]
56. Liu, Y.S.; Hu, Z.C.; Gao, S.; Günther, D.; Xu, J.; Gao, C.G.; Chen, H.H. In situ analysis of major and trace elements of anhydrous minerals by LA-ICP-MS without applying an internal standard. *Chem. Geol.* **2008**, *257*, 34–43. [[CrossRef](#)]
57. Liu, Y.S.; Gao, S.; Hu, Z.C.; Gao, C.G.; Zong, K.Q.; Wang, D.B. Continental and oceanic crust recycling-induced melt-peridotite interactions in the Trans-North China Orogen: U-Pb dating, Hf isotopes and trace elements in zircons of mantle xenoliths. *J. Petrol.* **2010**, *51*, 537–571. [[CrossRef](#)]

58. Liu, Y.S.; Hu, Z.C.; Zong, K.Q.; Gao, C.G.; Gao, S.; Xu, J.; Chen, H.H. Reappraisal and refinement of zircon U-Pb isotope and trace element analyses by LA-ICP-MS. *Chin. Sci. Bull.* **2010**, *55*, 1535–1546. [[CrossRef](#)]
59. Hu, Z.C.; Liu, Y.S.; Gao, S.; Xiao, S.Q.; Zhao, L.S.; Günther, D.; Li, M.; Zhang, W.; Zong, K.Q. A “wire” signal smoothing device for laser ablation inductively coupled plasma mass spectrometry analysis. *Spectrochim. Acta* **2012**, *78*, 50–57. [[CrossRef](#)]
60. Liu, Y.S.; Zong, K.Q.; Kelemen, P.B.; Gao, S. Geochemistry and magmatic history of eclogites and ultramafic rocks from the Chinese continental scientific drill hole: Subduction and ultrahigh-pressure metamorphism of lower crustal cumulates. *Chem. Geol.* **2008**, *247*, 133–153. [[CrossRef](#)]
61. Wiedenbeck, M.; Alle, P.; Corfu, F.; Griffin, W.L.; Meier, M.; Oberli, F.; Quadt, A.V.; Roddick, J.C.; Spiegel, W. Three natural zircon standards for U-Th-Pb, Lu-Hf, trace element and REE analyses. *Geostand. Geoanal. Res.* **1995**, *19*, 1–23. [[CrossRef](#)]
62. Compston, W.; Williams, I.S.; Kirschvink, J.L.; Zhang, Z.; Ma, G. Zircon U-Pb ages for the early cambrian time-scale. *J. Geol. Soc.* **1992**, *149*, 171–184. [[CrossRef](#)]
63. Ludwig, K.R. *User's Manual for Isoplot 3.00: A Geochronological Toolkit for Microsoft Excel*; Berkeley Geochronology Center: Alameda, Berkeley, CA, USA, 2003; Volume 39.
64. Li, X.H.; Li, Z.X.; Wingate, M.T.D.; Chung, S.L.; Liu, T.; Lin, G.C.; Li, W.X. Geochemistry of the 755 Ma Mundine Well dyke swarm, northwestern Australia: Part of a Neoproterozoic mantle superplume beneath Rodinia? *Precambrian Res.* **2006**, *146*, 1–15. [[CrossRef](#)]
65. Sircombe, K.N. Tracing provenance through the isotope ages of littoral and sedimentary detrital zircon, eastern Australia. *Sediment. Geol.* **1999**, *124*, 47–67. [[CrossRef](#)]
66. Nesbitt, H.W.; Young, G.M. Early Proterozoic climates and plate motions inferred from major element chemistry of lutites. *Nature* **1982**, *299*, 715–717. [[CrossRef](#)]
67. Nesbitt, H.W.; Young, G.M. Prediction of some weathering trends of plutonic and volcanic rocks based on thermodynamic and kinetic considerations. *Geochim. Cosmochim. Acta* **1984**, *48*, 1523–1534. [[CrossRef](#)]
68. Fedo, C.M.; Nesbitt, H.W.; Young, G.M. Unraveling the effects of potassium metasomatism in sedimentary rocks and paleosols, with implications for paleo-weathering conditions and provenance. *Geology* **1995**, *23*, 921–924. [[CrossRef](#)]
69. Cox, R.; Lowe, D.R. A conceptual review of regional-scale controls on the composition of clastic sediment and the co-evolution of continental blocks and their sedimentary cover. *J. Sediment. Res.* **1995**, *65*, 1–12.
70. Cox, R.; Lowe, D.R.; Cullers, R.L. The influence of sediment recycling and basement composition on evolution of mudrock chemistry in the southwestern United States. *Geochim. Cosmochim. Ac.* **1995**, *59*, 2919–2940. [[CrossRef](#)]
71. Boynton, W.V. Cosmochemistry of the rare earth elements: Meteorite studies dev. *Geochemistry* **1984**, *2*, 63–114.
72. Haskin, M.A.; Haskin, L.A. Rare earths in European shales redetermination. *Science* **1966**, *154*, 507–509. [[CrossRef](#)]
73. Taylor, S.R.; McLennan, S.M. *The Continental Crust: Its Composition and Evolution: An Examination of the Geochemical Record Preserved in Sedimentary Rocks*; Blackwell Scientific Publication: Oxford London, UK, 1985.
74. Wu, F.Y.; Zhao, G.C.; Wilde, S.A.; Sun, D.Y. Nd isotopic constraints on crustal formation in the North China Craton. *J. Asian Earth Sci.* **2005**, *24*, 523–545. [[CrossRef](#)]
75. Wu, F.Y.; Zhang, Y.B.; Yang, J.H.; Xie, L.W.; Yang, Y.H. Zircon U-Pb and Hf isotopic constraints on the Early Archean crustal evolution in Anshan of the North China Craton. *Precambrian Res.* **2008**, *167*, 339–362. [[CrossRef](#)]
76. Diwu, C.R.; Sun, Y.; Lin, C.L.; Liu, X.M.; Wang, H.L. Zircon U-Pb ages and Hf isotopes and their geological significance of Yiyang TTG gneisses from Henan province. *China. Acta Petrol. Sin.* **2007**, *23*, 253–262, (in Chinese with English abstract).
77. Diwu, C.R.; Sun, Y.; Yuan, H.L.; Wang, H.L.; Zhong, X.P.; Liu, X.M. U-Pb ages and Hf isotopes for detrital zircons from quartzite in the Paleoproterozoic Songshan Group on the southwestern margin of the North China Craton. *Chin. Sci. Bull.* **2008**, *53*, 2828–2839. [[CrossRef](#)]
78. Dong, M.M.; Wang, C.M.; Santosh, M.; Shi, K.X.; Du, B.; Chen, Q.; Zhu, J.X.; Liu, X.J. Geochronology and petrogenesis of the Neoproterozoic-Paleoproterozoic Taihua Complex, NE China: Implications for the evolution of the North China Craton. *Precambrian Res.* **2020**, *346*, 105792. [[CrossRef](#)]
79. Zhao, G.C.; Wilde, S.A.; Sun, M.; Guo, J.H.; Kröner, A.; Li, S.Z.; Li, X.P.; Wu, C.M. SHRIMP U-Pb zircon geochronology of the Huaian Complex: Constraints on Late Archean to Paleoproterozoic crustal accretion and collision of the Trans-North China Orogen. *Am. J. Sci.* **2008**, *308*, 270–303. [[CrossRef](#)]
80. Wu, M.L.; Zhao, G.C.; Sun, M.; Yin, C.Q.; Li, S.Z.; Tam, P.Y. Petrology and P-T path of the Yishui mafic granulites: Implications for tectonothermal evolution of the Western Shandong Complex in the Eastern Block of the North China Craton. *Precambrian Res.* **2012**, *222*, 312–324. [[CrossRef](#)]
81. Wu, M.L.; Zhao, G.C.; Sun, M.; Li, S.Z.; He, Y.H.; Bao, Z. Zircon U-Pb geochronology and Hf isotopes of major lithologies from the Yishui Terrane: Implications for the crustal evolution of the Eastern Block, North China Craton. *Lithos* **2013**, *170*, 164–178. [[CrossRef](#)]
82. Wu, S.J.; Hu, J.M.; Ren, M.H.; Gong, W.B.; Liu, Y.; Yan, J.Y. Petrography and zircon U-Pb isotopic study of the Bayanwulashan Complex: Constrains on the Paleoproterozoic evolution of the Alxa Block, westernmost North China Craton. *J. Asian Earth Sci.* **2014**, *94*, 226–239. [[CrossRef](#)]
83. Zhao, T.P.; Zhang, Z.H.; Zhou, Y.Y.; Wang, S.Y.; Liu, C.S.; Liang, H.J.; Zhang, B.C.; Hu, G.H. *Precambrian Geology of the Songshan Area, Henan Province*; Geological Publishing House: Beijing, China, 2012; pp. 1–206, (In Chinese with English abstract).

84. Zhai, M.G.; Bian, A.G. Amalgamation of the supercontinent of the North China Craton and its break up during late-middle Proterozoic. *Sci. China (D)* **2001**, *43*, 219–232. [[CrossRef](#)]
85. Kusky, T.M. Geophysical and geological tests of tectonic models of the North China Craton. *Gondwana Res.* **2011**, *20*, 26–35. [[CrossRef](#)]
86. Diwu, C.R.; Sun, Y.; Guo, A.L.; Wang, H.L.; Liu, X.M. Crustal growth in the North China Craton at ~2.5 Ga: Evidence from in situ zircon U-Pb ages, Hf isotopes and whole-rock geochemistry of the Dengfeng complex. *Gondwana Res.* **2011**, *20*, 149–170. [[CrossRef](#)]
87. Zhou, Y.Y.; Zhao, T.P.; Wang, C.Y.; Hu, G.H. Geochronology and geochemistry of 2.5 to 2.4 Ga granitic plutons from the southern margin of the North China Craton: Implications for a tectonic transition from arc to post-collisional setting. *Gondwana Res.* **2011**, *20*, 171–183. [[CrossRef](#)]
88. Wang, X.; Huang, X.L.; Yang, F.; Luo, Z.X. Late Neoarchean magmatism and tectonic evolution recorded in the Dengfeng Complex in the southern segment of the Trans-North China Orogen. *Precambrian Res.* **2017**, *302*, 180–197. [[CrossRef](#)]
89. Zhang, J.; Zhang, H.F.; Li, L.; Wang, J.L. Neoarchean-Paleoproterozoic tectonic evolution of the southern margin of the North China Craton: Insights from geochemical and zircon U-Pb-Hf-O isotopic study of metavolcanic rocks in the Dengfeng complex. *Precambrian Res.* **2018**, *318*, 103–121. [[CrossRef](#)]
90. Liu, C.H.; Zhao, G.C.; Sun, M.; Zhang, J.; Yin, C.Q.; He, Y.H. Detrital zircon U-Pb dating, Hf isotopes and whole-rock geochemistry from the Songshan Group in the Dengfeng Complex: Constraints on the tectonic evolution of the Trans-North China Orogen. *Precambrian Res.* **2012**, *192–195*, 1–15. [[CrossRef](#)]
91. Guo, J.H.; Sun, M.; Zhai, M.G. Sm-Nd and SHRIMP U-Pb zircon geochronology of high-pressure granulites in the Sanggan area, North China Craton: Timing of Paleoproterozoic continental collision. *J. Asian Earth Sci.* **2005**, *24*, 629–642. [[CrossRef](#)]
92. Zhang, J.; Zhao, G.C.; Li, S.Z.; Sun, M.; Wilde, S.A.; Liu, S.W.; Yin, C.Q. Polyphase deformation of the Fuping Complex, Trans-North China Orogen: Structures, SHRIMP U-Pb zircon ages and tectonic implications. *J. Struct. Geol.* **2009**, *31*, 177–193. [[CrossRef](#)]
93. Lu, J.S.; Wang, G.D.; Wang, H.; Chen, H.X.; Wu, C.M. Metamorphic P-T-t paths retrieved from the amphibolites, Lushan terrane, Henan Province and reappraisal of the Paleoproterozoic tectonic evolution of the Trans-North China Orogen. *Precambrian Research* **2013**, *238*, 61–77. [[CrossRef](#)]
94. Yang, Q.Y.; Santosh, M. Paleoproterozoic arc magmatism in the North China Craton: No Siderian global plate tectonic shutdown. *Gondwana Res.* **2015**, *28*, 82–105. [[CrossRef](#)]
95. Yang, Q.Y.; Santosh, M. Charnockite magmatism during a transitional phase: Implications for Late Paleoproterozoic ridge subduction in the North China Craton. *Precambrian Res.* **2015**, *261*, 188–216. [[CrossRef](#)]
96. Herron, M.M. Geochemical classification of terrigenous sands and shales from core or log data. *J. Sediment. Res.* **1988**, *58*, 820–829.
97. Nance, W.B.; Taylor, S.R. Rare earth element patterns and crustal evolution-I. Australian post—Archean sedimentary rocks. *Geochim. Et Cosmochim. Acta* **1976**, *40*, 1539–1551. [[CrossRef](#)]
98. Bhatia, M.R. Rare earth element geochemistry of Australian Paleozoic graywackes and mudrocks: Provenance and tectonic control. *Sediment. Geol.* **1985**, *45*, 97–113. [[CrossRef](#)]
99. Murray, R.W. Chemical criteria to identify the depositional environment of chert: General principles and applications. *Sedimentary Geol.* **1994**, *90*, 213–232. [[CrossRef](#)]
100. Mao, G.Z.; Liu, C.Y. Application of Geochemistry in Provenance and Depositional Setting Analysis. *J. Earth Sci. Environ.* **2011**, *33*, 337–348, (In Chinese with English abstract).
101. McLennan, S.M.; Hemming, S.; McDaniell, D.K.; Hanson, G.N. Geochemical approaches to sedimentation, provenance, and tectonics. *Geol. Soc. Am. Spec. Pap.* **1993**, *284*, 21–40.
102. Allegre, C.J.; Minster, J.F. Quantitative models of trace element behavior in magmatic processes. *Earth Planet. Sci. Lett.* **1978**, *38*, 1–25. [[CrossRef](#)]
103. Floyd, P.A.; Leveridge, B.E. Tectonic environment of the Devonian Gramscatho basin, south Cornwall: Framework mode and geochemical evidence from turbiditic sandstones. *J. Geol. Soc.* **1987**, *144*, 531–542. [[CrossRef](#)]
104. Condie, K.C. Chemical composition and evolution of the upper continental crust: Contrasting results from surface samples and shales. *Chemical geology* **1993**, *104*, 1–37. [[CrossRef](#)]
105. Zhao, T.P.; Jin, C.W. Review on the study of the Xiong'er Group in past 40 years. *North China J. Geol. Miner. Resour.* **1999**, *14*, 18–26, (In Chinese with English abstract).
106. Zhao, T.P.; Wang, J.P.; Zhang, Z.H. *Proterozoic Geology of Mt. Wangwushan Mountain and Adjacent Areas*; China Land Press: Beijing, China, 2005. (In Chinese)
107. Bhatia, M.R.; Crook, K.A.W. Trace element characteristics of graywackes and tectonic setting discrimination of sedimentary basins. *Contrib. Mineral. Petrol.* **1986**, *92*, 181–193. [[CrossRef](#)]
108. Bhatia, M.R. Plate tectonics and geochemical composition of sandstones. *J. Geol.* **1983**, *91*, 611–627. [[CrossRef](#)]
109. Bhatia, M.R.; Taylor, S.R. Trace-element geochemistry and sedimentary provinces: A study from the Tasman Geosyncline, Australia. *Chem. Geol.* **1981**, *33*, 115–125. [[CrossRef](#)]
110. Xu, Y.J.; Du, Y.S.; Yang, J.H.; Huang, H. Sedimentary geochemistry and provenance of the lower and middle Devonian Laojunshan Formation, the north Qilian orogenic belt. *Sci. China Earth Sci.* **2010**, *53*, 356–367. [[CrossRef](#)]

111. Wang, W.; Zhou, M.F.; Yan, D.P.; Li, J.W. Depositional age, provenance, and tectonic setting of the Neoproterozoic Sibao Group, Southeastern Yangtze Block, South China. *Precambrian Res.* **2012**, *192–195*, 107–124. [[CrossRef](#)]
112. Zhang, M.; Liu, Z. Geochemistry of pelitic rocks from the Middle Permian Lucaogou Formation, Sangonghe area, Junggar basin, Northwest China: Implications for source weathering, recycling, provenance and tectonic setting. *Geol. J.* **2015**, *50*, 552. [[CrossRef](#)]

Disclaimer/Publisher’s Note: The statements, opinions and data contained in all publications are solely those of the individual author(s) and contributor(s) and not of MDPI and/or the editor(s). MDPI and/or the editor(s) disclaim responsibility for any injury to people or property resulting from any ideas, methods, instructions or products referred to in the content.